Quaternary Science Reviews 225 (2019) 105894

Contents lists available at ScienceDirect

Quaternary Science Reviews

journal homepage: www.elsevier.com/locate/quascirev

A new varve sequence from Windermere, UK, records rapid ice retreat prior to the Lateglacial Interstadial (GI-1)

Rachael S. Avery [a, *], Alan E.S. Kemp [a], Jonathan M. Bull [a], Richard B. Pearce [a], Mark E. Vardy [a, 1], J. James Fielding [a, 2], Carol J. Cotterill [b]

[a] Ocean and Earth Science, University of Southampton, National Oceanography Centre, Southampton, Southampton, SO14 3ZH, United Kingdom
[b] British Geological Survey, Lyell Centre, Research Avenue South, Edinburgh, EH14 4AP, United Kingdom

ARTICLE INFO

Article history:
Received 13 November 2018
Received in revised form
19 August 2019
Accepted 21 August 2019
Available online 18 October 2019

Keywords:
Pleistocene
Palaeolimnology
Glaciation
Western Europe
Sedimentology (lakes)
Varves
British-Irish ice sheet
Lateglacial
Heinrich Stadial 1
Bølling-Allerød

ABSTRACT

Annually laminated sediments (varves) provide excellent temporal resolution to study rapid environmental change, but are rare in the early part of the Last Termination (~19–~11.7 ka BP). We present a new >400 varve year (vyr) varve sequence in two floating parts from Windermere, a lake at the southern margin of the mountains of northwest England. This sequence records the final retreat of the Windermere glacier at the southern edge of the Lake District Ice Cap during the transition from Heinrich Stadial 1 (~18–~14.7 ka BP) into the Lateglacial Interstadial (~14.7–~12.9 ka BP).

Laminated sediments from four lake cores from Windermere's northern and southern basins were investigated and shown to be varved. These sequences are integrated with seismic reflection evidence to reconstruct south-to-north deglaciation. Seismic and sedimentological evidence is consistent with gradual stepped ice retreat along the entire southern basin and into the northern basin between 255 and 700 vyr prior to the appearance of significant biota in the sediment that heralded the Lateglacial Interstadial, and had retreated past a recessional moraine (RM8) in the northern basin by 121 vyr prior to the interstadial. The Lateglacial Interstadial age of this biota-bearing unit was confirmed by ^{14}C-dating, including one date from the northernmost core of ~13.5 cal ka BP. A change in mineralogy in all four cores as the glacier retreated north of the Dent Group (the northernmost source of calcareous bedrock) and a decrease in coarse grains in the varves shows that the ice had retreated along the entire North Basin at ~70 vyr prior to the Lateglacial Interstadial. The estimated retreat rate is 70–114 m yr^{-1} although buried De Geer moraines, if annual, may indicate retreat of 120 m yr^{-1} with a ≥3 year stillstand at a recessional moraine halfway along the basin. The glacier then retreated north of the lake basin, becoming land-terminating and retreating at 92.5–49 m yr^{-1}.

The northernmost core has a varve sequence ending at least 111 vyr after the other core chronologies, due to the increased proximity to remnant ice in the catchment uplands into the early Lateglacial Interstadial. We show that almost all of the glacier retreat in the Windermere catchment occurred before the abrupt warming at the onset of the Lateglacial Interstadial, in keeping with similar findings from around the Irish Sea Basin, and suggesting a similar retreat timescale for other radial valley glaciers of the Lake District Ice Cap. The seismic and core evidence also show the potential for a much longer varve chronology extending at least 400 and potentially over 1000 vyr further back into Heinrich Stadial 1 (18–14.7 ka BP), suggesting that glacier retreat in the Windermere valley initiated at least before 15.5 ka BP and perhaps 16 ka BP.

* Corresponding author. Present address: Department of Geological sciences, Stockholm University, SE-10691, Stockholm, Sweden.
E-mail addresses: rachael.avery@geo.su.se (R.S. Avery), aesk@noc.soton.ac.uk (A.E.S. Kemp), bull@noc.soton.ac.uk (J.M. Bull), r.pearce@noc.soton.ac.uk (R.B. Pearce), mark.vardy@sandgeophysics.com (M.E. Vardy), jjf1e13@soton.ac.uk (J.J. Fielding), cjcott@bgs.ac.uk (C.J. Cotterill).
[1] Present address: SAND Geophysics, 44 Chatsworth Road, Southampton, United Kingdom, SO19 7NJ.
[2] Present address: Geography and Environmental Science, University of Southampton, University Road, Southampton, United Kingdom, SO17 1BJ

https://doi.org/10.1016/j.quascirev.2019.105894

1. Introduction

Understanding the pattern and timing of ice retreat after the global Last Glacial Maximum (LGM; 26.5–20 ka BP; Clark et al., 2009) is an ongoing question that has implications for the effects of anthropogenic global warming. The British-Irish Ice Sheet (BIIS) in particular has enjoyed a long history of research (e.g. Agassiz, 1840; Buckland, 1840), recently with a strong focus on constructing reliable retreat chronologies for its different sectors (Ó Cofaigh et al., 2019; Roberts et al., 2018; Small et al., 2017a; Smedley et al., 2017b, 2017a). We know from the annually resolved chronology of the Greenland ice-core records that several major climate shifts post-LGM occurred on decadal timescales (Rasmussen et al., 2006; Steffensen et al., 2008), including the onset of the Lateglacial Interstadial (~14.7–~12.9 ka BP; Greenland Interstadial 1, Bølling-Allerød Interstadial, Windermere Interstadial) 14,642 ± 4 yr BP. Varved or annually laminated lake sediments possess a temporal resolution directly comparable to the ice-core records and may be used to quantify the duration of climatic intervals and also to establish the rates of environmental change within them, including ice retreat (Ojala et al., 2012; Zolitschka et al., 2015). The formation of varves is relatively uncommon, requiring both strong seasonality of one or more depositional processes, and preservation of lakebed microstructure with little to no bioturbation (Zolitschka, 2007). Varves in glacial climates are usually clastic, comprising a 'summer' (melt season) coarse graded layer derived from glacial or nival meltwater, and a fine 'winter' clay cap formed by settling from suspension. In a proglacial environment, varve thickness is controlled by the level of meltwater production from catchment ice masses, such that thicker varves usually indicate more melting degree-days during a given year (Ridge et al., 2012). Annually-resolved ice retreat chronologies have been constructed using varve chronologies in e.g. Sweden (Holmquist and Wohlfarth, 1998, and references therein), North America (Ridge et al., 2012) and Patagonia (Bendle et al., 2017).

In 1943, Winifred Pennington discovered mm-scale clay laminations below the 'brown mud' (i.e. the Holocene sediment) in her cores from Windermere, UK, and tentatively identified them as varves (Pennington, 1943), even suggesting later (Pennington, 1947) that they could be correlated with the varves of De Geer's Swedish Varve Chronology (e.g. De Geer, 1937, 1912). Although her initial interpretations that these mm-scale varves formed during the deglaciation of the catchment (Pennington, 1943) were not correct (the varves she referred to were of Younger Dryas age, later shown to post-date initial deglaciation), she also mentioned the presence of some 'lower laminated clays'. In 1947 she expanded on this, describing the lower laminations as much thicker (up to 1 cm) but thinning into mm-scale laminations that eventually disappeared as the sediment transitioned to a 'grey layer' (Pennington, 1947). The 'grey layer' was attributed to the Allerød and would later form the basis for Windermere becoming the type site for the 'Windermere' Interstadial in Britain (Coope and Pennington, 1977). The lower laminations were attributed to the 'lower' Dryas and initial deglaciation of the catchment, and the upper laminations to the 'upper' Dryas (Pennington, 1947). Whilst many of the details and dates were refined later (e.g. Coope and Pennington, 1977; Knight, 2001), that basic stratigraphy and interpretation of cold deglaciation - warm - cold were essentially correct.

Since Pennington's research, few Lateglacial-aged (~14.7–11.7 ka BP) varved chronologies have been found in the UK (Devine and Palmer, 2017; Palmer et al., 2012, 2010), and fewer still from the earlier part of the deglaciation (~20 ka BP-14.7 ka BP, Livingstone et al., 2010b; Palmer et al., 2008). In the case of the Solway Lowlands (just to the north-east of the Lake District) varves were used to infer the presence of a proglacial palaeo-lake that existed for at least 261 years (Livingstone et al., 2010b). In southern Wales, the existence of palaeo-lake Llangorse was already known, but varve facies and thicknesses were utilised to infer sedimentary processes in the proglacial lake as the valley glacier retreated. Pennington inferred from the presence of the varves in Windermere that glacial retreat had occurred (Pennington, 1947, 1943), but did not have enough 'lower laminated clays' to produce a substantial deglacial chronology.

Here we present a new >400 varve year (vyr) pre-Lateglacial Interstadial varve sequence in two floating parts from Windermere in the Lake District of northwest England, in the context of the shrinking Lake District Ice Cap (LDIC) during the deglaciation of the British and Irish Isles immediately prior to the Lateglacial Interstadial (Clark et al., 2012; Hughes et al., 2014; Livingstone et al., 2015). Working on new radiocarbon-dated deep-water piston cores from Windermere, we have applied a suite of techniques including image-based (optical and SEM), geochemical, and grain size measurement, and integrated this with previous geophysical survey results, to reconstruct the sedimentary history of the Windermere catchment prior to the Lateglacial Interstadial. Several varve sequences from the lake basin, equivalent to Pennington's 'lower laminated clays', have been identified and used to shed light on the nature of the retreat of the valley glacier from the Windermere catchment. We demonstrate the potential of UK lakes to provide pre-Lateglacial Interstadial varved sediments that may be used to further constrain ice sheet retreat timings and rates, and potentially to provide long, annually-resolved archives for proxy-based palaeoclimate reconstruction.

2. Study location

2.1. Windermere

Windermere is a north-south trending glacial ribbon lake in the southeast of the English Lake District (Fig. 1), lying in a steep-sided pre-glacial river valley that has been overdeepened by successive glaciations (Pennington, 1973; Pinson et al., 2013). The lake has a present maximum water depth of 62 m and an elevation of 39 m above Ordnance Datum Newlyn. It has maximum dimensions of 17 km × 1.5 km and drains a catchment of 242 km^2 (Lowag et al., 2012; Miller et al., 2013). The catchment bedrock comprises the Ordovician Borrowdale Volcanic Group in the north and the Windermere Supergroup (Silurian mudstones and siltstones) in the south. The lake is separated into north and south basins by a bedrock high, with the South Basin draining westward into the River Leven (Wilson, 1987).

Windermere has been the subject of much research over the last several decades, from Lateglacial stratigraphy (e.g. Pennington, 1947, 1943), to palaeomagnetic secular variation (e.g. Avery et al., 2017; Turner and Thompson, 1981), to pollution and environmental degradation (e.g. McGowan et al., 2012; Miller et al., 2014b), and is the home of the Freshwater Biological Association in Britain. Much of the research done by Winifred Pennington from the 1930's to the 1970's concerned the diatoms, pollens, and varves of the Lateglacial period (e.g. Coope and Pennington, 1977; Pennington, 1977, 1947, 1943). Additionally, the manifestation of the Lateglacial Interstadial in Britain is historically known as the Windermere Interstadial on account of Windermere being its type site (Coope and Pennington, 1977).

2.2. British-Irish Ice Sheet (BIIS) retreat in the region

During the LGM three semi-independent ice sheets in northern Europe (the British-Irish; Scandinavian, and Svalbard-Barents-

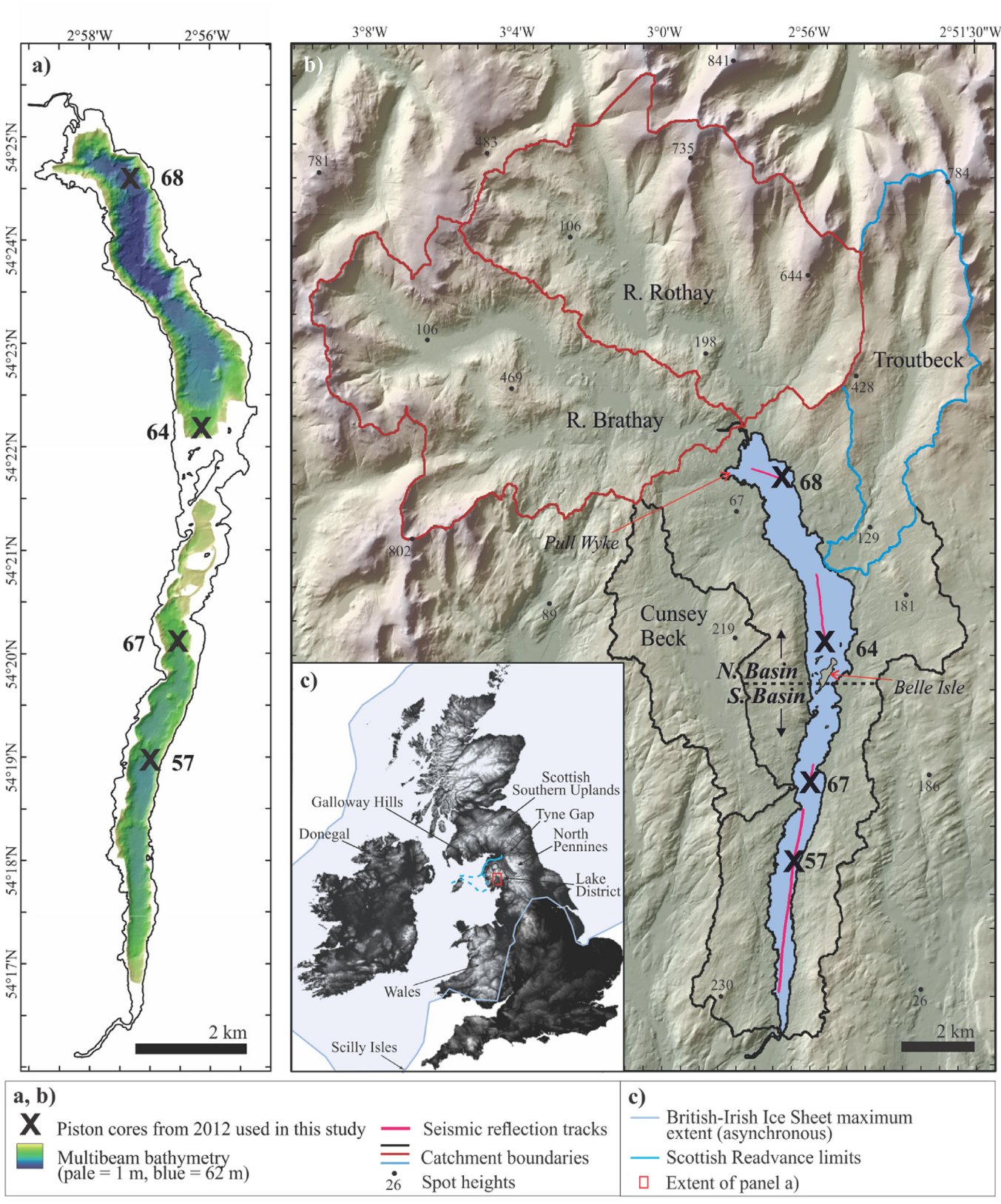

Fig. 1. Map of the study area. a) Multibeam bathymetry of Windermere with core locations. b) The lake catchment of Windermere is shown in bold outlines (significant sub-catchments are shown in red and blue). Significant fluvial inputs to the lake are named in the catchments. Topography derived from 1- and 2 m LiDAR datasets and NEXTMap data; spot heights are from Ordnance Survey. The locations of the four studied cores are shown as black crosses. Seismic lines that form the multichannel seismic reflection sections in Fig. 2 are shown as pink lines. Multibeam lake bathymetry is shown as a half-rainbow colour palette, where dark blue is deepest. The north and south lake basins are separated by a black dashed line, and the location of the largest island, Belle Isle, is indicated with a red arrow. c) The location of Windermere (red rectangle) in the British and Irish Isles. Pale blue and bright blue lines show the maximum British-Irish Ice Sheet extent and possible extent of the Scottish Readvance ice respectively (after Chiverrell et al., 2018; A. L. C. Hughes et al., 2016a; Livingstone et al., 2010a). Contains SRTM data. Contains Ordnance Survey data © Crown copyright and database right 2017, and UK Environment Agency data © Environment Agency copyright and/or database right 2015. All rights reserved. (For interpretation of the references to colour in this figure legend, the reader is referred to the Web version of this article.)

Kara) reached their maximum extents, coalescing into a single Eurasian ice sheet complex around 25 ka BP (A. L. C. Hughes et al., 2016a). After ~20 ka BP, retreat and break-up of the ice sheet complex was strongly asynchronous as different sectors were subject to regional variation in response to climate forcing and internal ice dynamics (Clark et al., 2012; Patton et al., 2017).

The maximum extents of different sectors of this ice sheet complex occurred at different times over the broad LGM period (A. L. C. Hughes et al., 2016a). The BIIS maximum extent in the southern and western sector was reached around 26–25 ka BP (early in Heinrich Stadial 2, ~26–24 ka BP), when the large Irish Sea Ice Stream extended to the Scilly Isles (Smedley et al., 2017a,b, Fig. 1c) and possibly to the continental shelf edge (Praeg et al., 2015), drawing ice in its onset zone from sources peripheral to the northern Irish Sea Basin including north-east Ireland, south-west Scotland and north-west England. Around 24 ka BP the Irish Sea Ice Stream had already rapidly retreated north of the Scilly Isles to northern Wales (Glasser et al., 2018; Smedley et al., 2017a). By 22 ka BP, ice surfaces were lowering, leading to more topographically-controlled ice flow in terrestrial sectors and some exposed bedrock prominences, for example in north and south Wales around 20–19 ka BP (Glasser et al., 2018; Hughes et al., 2014; P. D. Hughes et al., 2016b).

The northern Irish Sea Basin continued to draw down ice from its periphery, with Scottish and Lake District ice in fact readvancing at ~19.3–18.3 ka BP amongst minor oscillations (Chiverrell et al., 2018; Livingstone et al., 2010a, Fig. 1c), before subsequent retreat across the Solway Lowlands and separation of Lake District and Scottish ice sources. The deglaciation of the lowlands around the southeast of the Lake District also occurred just subsequent to this (Chiverrell et al., 2018, 2016). On the northern and eastern fringes of the Lake District, the Tyne Gap (northeast of the Lake District, between the North Pennines and Scottish Southern Uplands; Fig. 1c), partially fed by Lake District ice, became deglaciated by 16.4–15.7 ka BP, signalling final isolation of the LDIC from the remaining BIIS, which was thereafter confined to Scotland and the north of Ireland (Livingstone et al., 2015). This formed part of the gradual separation of the BIIS into isolated, locally-controlled, upland ice caps (Hughes et al., 2014).

Emergence of the upland Lake District from ice cover around 17 ka BP as ice surfaces lowered is suggested by a cosmogenic isotope age of 17.3 ± 1.1 ka BP from a 750 m col of Scafell Pike, the Lake District's highest peak (Ballantyne et al., 2009; Hughes et al., 2014). As well as thinning, the ice was also retreating up-valley towards the LDIC centre (Wilson and Lord, 2014). For example, Schmidt-Hammer exposure dating (Tomkins et al., 2017, 2016) and ^{10}Be exposure dating (Wilson et al., 2018) applied to granite surfaces at Shap Fell in eastern Cumbria show that the area became exposed at 16.5 ± 0.5 to 16.65 ± 1.36 ka BP respectively as ice retreated southwest into the eastern Lake District. On the other hand, valley exposure ages in the northern and western Lake District from erratic boulders and a roche moutonnée, and moraine boulders from the Duddon Valley to the west of Windermere, are interpreted to indicate the persistence of valley glaciers until around 15 ka BP or possibly later (Wilson et al., 2018). In this context, it is likely that the deglaciation of the Windermere valley also occurred during this period between 16 and 15 ka BP prior to, and possibly into, the rapid climate warming of the Lateglacial Interstadial at ~14.7 ka BP.

3. Seismic stratigraphy of sediments

Two-dimensional multichannel boomer seismic reflection surveys of Windermere reveal several distinct seismostratigraphic units (Table 1) above the bedrock (Pinson et al., 2013). The seismic reflection sections were prestack depth migrated to give depth rather than time sections and four major seismic units were interpreted. Seismic Facies I (SF I) is interpreted as over-consolidated till and morainic material, SF II as glaciolacustrine and lacustrine sedimentation prior to the Holocene, SF III as representing Younger Dryas –age mass movement complexes, and SF IV as the organic Holocene drape (Fig. 2). Some units (SFI and SFII) are further subdivided into minor units based on distribution, seismic architecture and interval seismic velocity.

Within SF I, Pinson et al. (2013) interpreted a sequence of 9 recessional moraines (RMs) and 28 De Geer moraines (DGMs) preserved beneath the modern lakebed (Fig. 3). RMs are interpreted to represent localised still-stands or readvances, whilst DGMs can sometimes represent annual retreat formations (Bouvier et al., 2015). Seven out of nine RMs are located in the South Basin, which suggests that ice retreated episodically in the narrow southern end of the valley. Melt-out till in two depocentres between recessional moraines 2–3 and 4–5 was interpreted by Pinson et al. (2013) as localised downwasting (Fig. 2). Only two RMs are in the North Basin, which instead has a wider valley structure and contains a series of at least 28 semi-regularly spaced De Geer moraines, which Pinson et al. (2013) interpret as a signature of much faster retreat than in the South Basin. The seismic and morphological interpretation of the deglaciation of Windermere is that of complex and active glacial retreat northwards along the valley with short still-stands or readvances, with deglaciation of the northern sub-catchments (Rothay and Brathay) occurring after those to the south (Cunsey Beck and Troutbeck; see Fig. 1) (Miller et al., 2014a; Pinson et al., 2013).

Table 1
Seismic stratigraphy of the sub-bottom Windermere sediments, following Pinson et al. (2013).

Seismic Facies	Seismic characterisation (average seismic interval velocity in brackets)	Sediment type as seen in available cores (see section 4.1)
SF IV	A 2- to 5-m-thick draped deposit, with several low-amplitude but continuous layered internal reflection. [~1490 m s^{-1}]	Organic-rich Holocene mud
SF III	Disturbed, erosive deposit with weak, chaotic internal reflections or discrete, transparent deposits with high-amplitude bounding reflection. [~1500 m s^{-1}]	Younger Dryas mass movement deposits (Examples may be found in the South Basin cores)
SF IIb	Unit with weak, closely spaced (<0.5 m) internal reflections, only observed in the South Basin. [1500 m s^{-1} + 6 m s^{-1} per metre]	Glaciolacustrine infill, relating to cm-scale laminations with a thickening trend downwards through the unit. This unit is only present in the South Basin.
SF IIa	Up to 35-m-thick deposit infilling the SF I topography with strong, layered internal reflections that widen with depth. Grades into the overlying SF IIb. [1500 m s^{-1} + 6 m s^{-1} per metre]	Glaciolacustrine infill, relating to cm- and mm-scale clay and silt laminations and homogenous Interstadial-age sediment. Sandier deposits towards the bases of the two North Basin cores may be transitional to SF I.
SF I	Complex unit with several sub-units and variable internal structure, bounded by strong top and bottom reflections. [2300 ± 300 −3500 ± 500 m s^{-1}]	A complex sequence of tills and moraines with localised flowed till and ice-proximal fan deposits, as well as an upper unit of supraglacial and melt-out till. No cores penetrated into this unit.

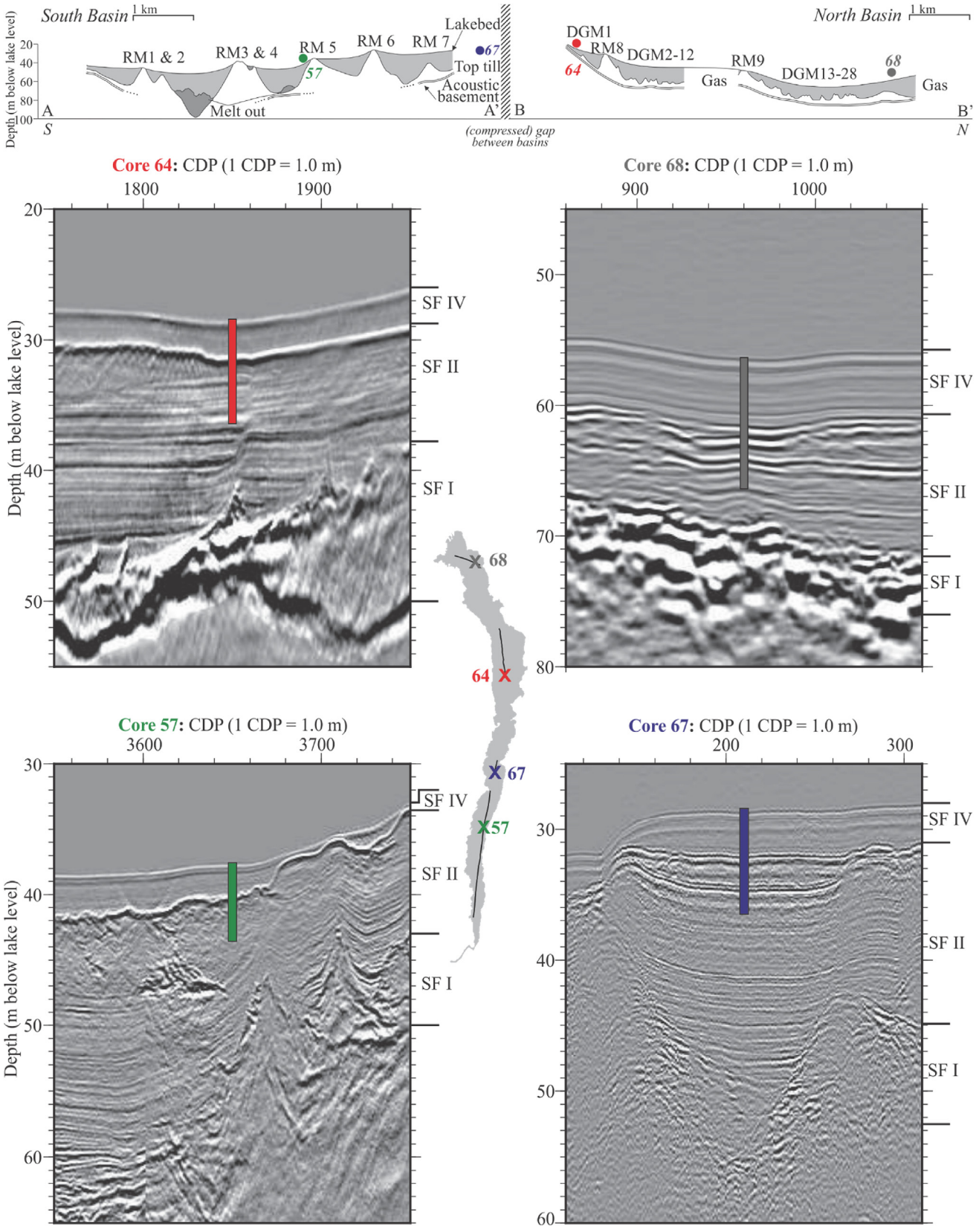

Fig. 2. Top: thalweg profiles down the South and North basins respectively with coloured circles showing core locations (vertical exaggeration 16:1); see Fig. 3 for thalweg locations. RM = recessional moraine; DGM = De Geer moraine. Adapted from Pinson et al. (2013), © John Wiley and sons. Bottom: multichannel seismic stratigraphy of the locations of all four studied cores (see Fig. 1 for locations): 64 (southern North Basin), 68 (northern North Basin), 57 (mid- South Basin), 67 (northern South Basin). Cores are shown as coloured vertical lines. Seismic facies SF I, II, and IV are shown with boundaries on the right.

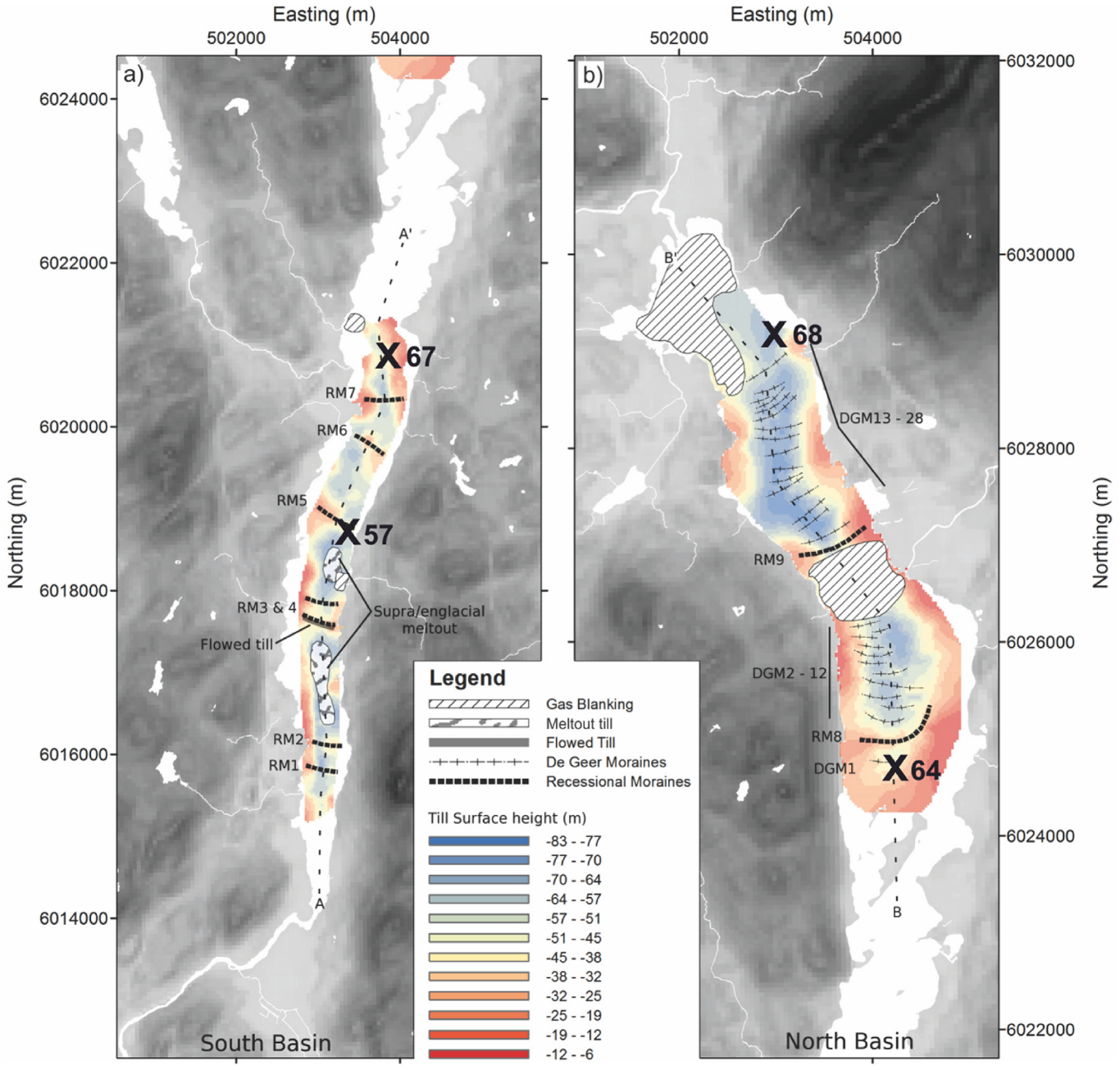

Fig. 3. Glaciogenic features present in Windermere. a, b) Extent of interpreted glaciogenic landforms within Windermere. The dashed black lines A-A′ and B-B′ indicate the thalweg profile locations (Fig. 2). Core locations are shown as black X's. After Pinson et al. (2013), © John Wiley and sons.

4. Methods

4.1. Sediment coring

The multichannel boomer seismic reflection data, together with chirp, parametric subbottom profiler and multibeam bathymetry data, collected between 2007 and 2011 by the University of Southampton and the British Geological Survey, were collectively used to select a series of locations in sediment depocentres for piston coring (Lowag et al., 2012; Miller et al., 2013; Pinson, 2009; Pinson et al., 2013; Vardy et al., 2010, Fig. 3). A coring campaign in 2012 by the British Geological Survey (BGS) and the University of Southampton facilitated the collection of several sediment cores using both a Uwitec piston corer and Uwitec gravity corer (Miller, 2014). The four cores with the highest deposition rates and covering the longest time intervals were selected for this detailed study (+54–03/57 PC, +54–03/67 PC, +54–03/64 PC, and +54–03/68 PC; hereafter 'Core 57', 'Core 67, 'Core 64, and 'Core 68' respectively; Fig. 1; Fig. 2). Overlapping cores were not taken, so there is a short (<10 cm) core gap between each 2 m cored section. The 2012 piston coring did not recover the sediment-water interface, so short gravity cores were subsequently taken in 2014 in order to recover the most recent sedimentation. The gravity core sequences were spliced into the piston core sequences, such that the piston cores do not start at 0 m depth (defined as the sediment-water interface).

4.2. Radiocarbon and radionuclide dating

Several radiocarbon dates were obtained from the Windermere cores. From the Holocene sediments, age models for Cores 57, 67, 64 and 68 were constructed using 4, 6, 5, and 9 reliable accelerator mass spectrometry (AMS) radiocarbon dates respectively (Avery et al., 2017). In addition to the Holocene, radiocarbon dates were obtained from the organic silty clay unit, which stratigraphically corresponded to the Lateglacial Interstadial. The dates were obtained from both macrofossils such as terrestrial leaves and twigs, and from 1 cm thick bulk sediment samples where macrofossils were not found. Macrofossils and sediment samples were preferentially taken from the split cores (excluding the top and bottom 10 cm to avoid contamination) using clean metal scalpels and spatulas, weighed, and stored in glass or metal containers. At the NERC Radiocarbon Facility in East Kilbride, Scotland, the samples were digested in 2 M HCl at 80 °C for 2 h, washed, dried and homogenised. The carbon was recovered as CO_2 by heating with CuO in a sealed quartz tube, then converted to graphite by Fe/Zn reduction. The graphite was then sent to the SUERC AMS laboratory for ^{14}C analysis (Charlotte Bryant, NERC Radiocarbon Facility, written communication). Dates were calibrated using Calib 7.1 (Stuiver and Reimer, 1993) and the Intcal13 calibration curve (Reimer et al., 2013).

A ^{210}Pb-decay age model was produced for each gravity and piston core, and the age models for the gravity cores were validated using ^{137}Cs bomb-testing and Chernobyl peaks (see Fielding et al., 2018 for procedural details). The ^{137}Cs-validated, ^{210}Pb-decay age model-derived date for the top of each piston core is given in Supplementary Table 1 and Fig. 5. A detailed radiocarbon dating table may be found in (Avery, 2017).

4.3. Sample processing, imaging, lamina measurement and counting

Split cores were sampled at the British Ocean Sediment Core Facility (BOSCORF), producing U-channels and 1×5 cm sediment slabs from the centre of the core. The U-channels were used for Itrax ED-XRF core scanning to identify geochemical variations downcore. The sediment slabs were X-radiographed and photographed for use as a digital archive, then subsampled to produce overlapping 3–4 cm covered (CTS) and polished (PTS) thin sections as well as subsamples for other techniques e.g. grain size analysis. In order to ascertain certain mineral compositions of parts of the sediment, energy-dispersive X-ray spectroscopy (EDS) maps were produced using the Scanning Electron Microscope (SEM). An additional X-ray diffraction method was employed on one sample from the bottom of Core 68 to identify constituent minerals. Grain sizes were also measured from representative samples of different sediment types.

Laminated clay-silt couplets were investigated to assess their annual nature in order to build a varve chronology and to understand better the style of sedimentation, and thus the catchment environment, in Windermere. Millimetre-scale and centimetre-scale lamina couplets were measured, and in the South Basin cores 57 and 67, distinctive 'marker' laminae were identified following the methods of Lamoureux (2001). A composite couplet chronology between the South Basin cores was therefore constructed using 16 well-correlated marker beds (see Supplementary Section 12.2). Cores 64 and 68 did not contain the same reference layers, and the couplets present in these cores were counted without cross-referencing.

Millimetre-scale laminations were measured from SEM backscatter images of PTS and from optical microscopy of CTS, whilst thicker laminations were measured from CIS images of the split core, alongside auxiliary X-radiographs (Fig. 4). In some cases, several methods were used in parallel for cross-checking. For all measurement methods, three vertical lines were drawn on the image and horizontal lines were drawn at each lamina couplet boundary. The lamina thicknesses were measured using the semi-automated method of Francus et al. (2002). The number of lamina couplets in each sequence was counted by two researchers, where a discrepancy was given as a $+1$ or -1 uncertainty. The error was calculated as the total absolute uncertainty as a percentage of the final count. In the case of Cores 57 and 67, correlated using marker beds, each core's count was re-appraised by comparison with equivalent sections of the other core (Tomkins et al., 2008).

A series of fifteen tills were collected from the Rothay/Brathay catchments (Fig. 1) in order to use Sr isotopes to ascertain the provenance of some calcium-bearing sediments found in the cores (since Sr often replaces Ca in minerals). One sample was also taken from each core where Itrax and SEM evidence indicated high-calcium areas. The tills were washed, then each till and core sample was placed in 10% nitric acid. The core samples effervesced, but the till samples did not, making them unsuitable for Sr analysis.

5. Results

5.1. Core stratigraphy

All four cores exhibit similar major lithological units (Fig. 5): an inorganic mineral-rich base overlain by a dark organic rich unit.

The base of the northernmost core (Core 68) exhibits disturbance with irregular laminations, deformation, and massive sand beds, overlain by several cm-scale alternating silt and clay laminations. The base unit for the other North Basin core (Core 64) comprises cm-dm-scale silt-clay laminations, which, although disturbed and deformed in places, also thin up-core into cm-scale and mm-scale laminations. The base unit in cores from the South Basin (Cores 57 and 67) begins with the cm-scale alternating silt and clay laminations, thinning up-core into mm-scale silt and clay laminations. The overlying unit in all cores is silty clay that contains diatoms (Core 67) and other organic matter (all cores), as well as ferric growths (Cores 57 and 68). This organic silty clay unit is succeeded by a unit of mm-scale laminated silt and clay which is interrupted, in the case of the South Basin cores, by mass transport deposits up to 1.5 m thick. The upper unit in all cores is a homogenous, dark, organic-rich mud.

5.2. ^{14}C dating

Radiocarbon dating indicates that the dark brown organic unit is of Holocene age, whilst the underlying sediment is pre-Holocene (Fig. 5). A stratigraphically coherent radiocarbon date (13422–13574 cal yr BP; 2σ) from near the top of the lower organic, silty clay unit in Core 68 (see Fig. 5) indicates that it is of Lateglacial Interstadial age and appears to be reliable. However, the dates sourced from the lowest part of the organic silty clay unit (median probabilities 18,459 cal yr BP from Core 68; 17,134 cal yr BP from Core 67) seem too old. Due to the absence of terrestrial microfossils in the lower interstadial sediments, our dates were obtained from bulk sediment and so were likely subject to a number of processes typical in deglacial environments that can lead to anomalously old dates. These may include the washing in of old carbon from the recently exposed ice-free terrain, and also reservoir effects such as the influence of old groundwater (Lowe and Walker, 2000; Small et al., 2017b). Similar discrepancies are typical in Northern European late glacial lake sediments (Blystad and Selsing, 1989; Wohlfarth, 1996) and in deglaciated environments in general (Hutchinson et al., 2004). If we assume the onset of organic

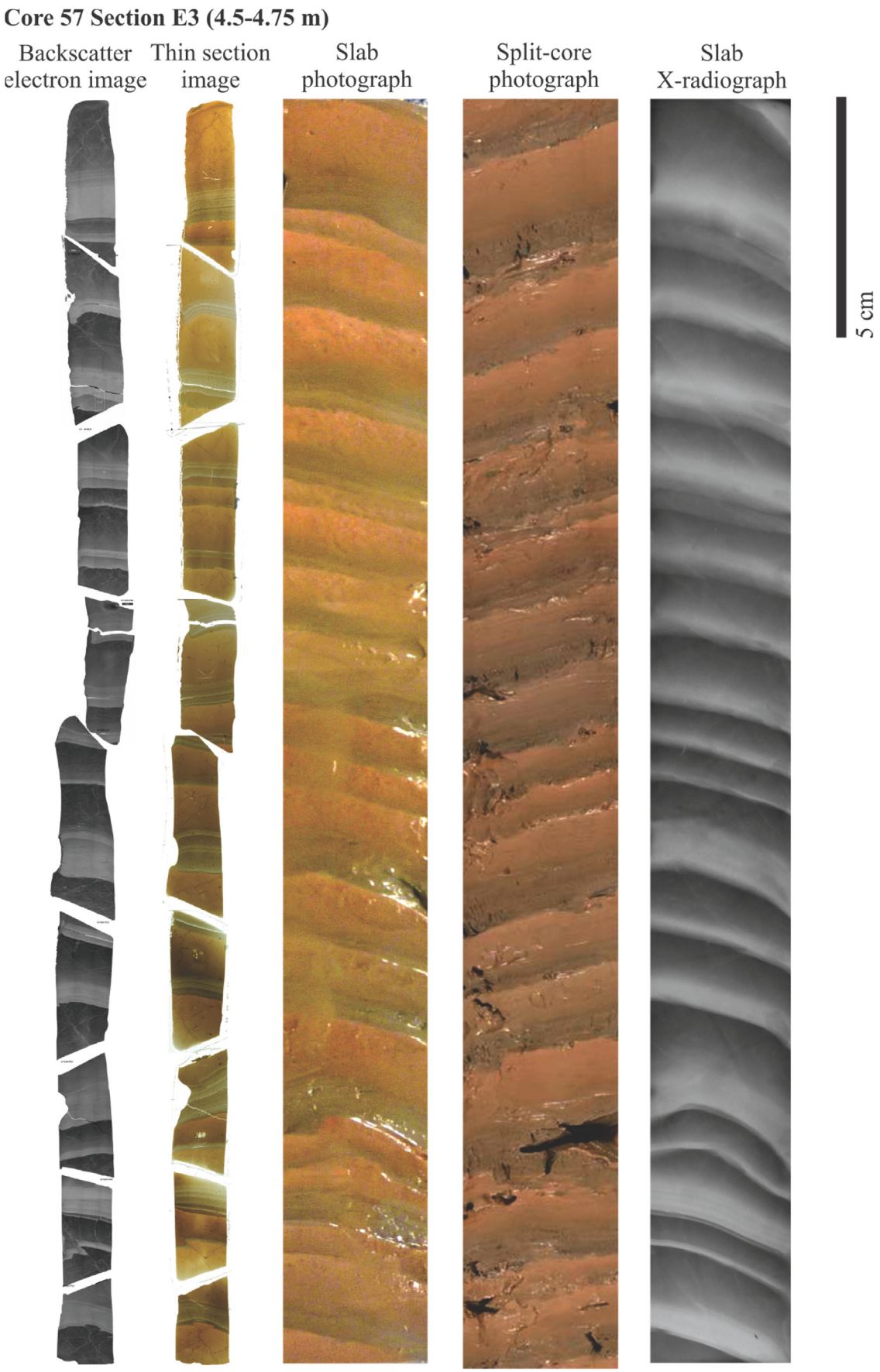

Fig. 4. Centimetre-scale laminations (facies CF III) from Core 57, 4.5–4.75 m, showing examples of the different imaging methods used in lamina couplet analysis and cross-checking. From left: BSEI of polished thin sections; Covered thin section optical photomicrographs; Slab photograph; Split-core photograph; Slab X-radiograph.

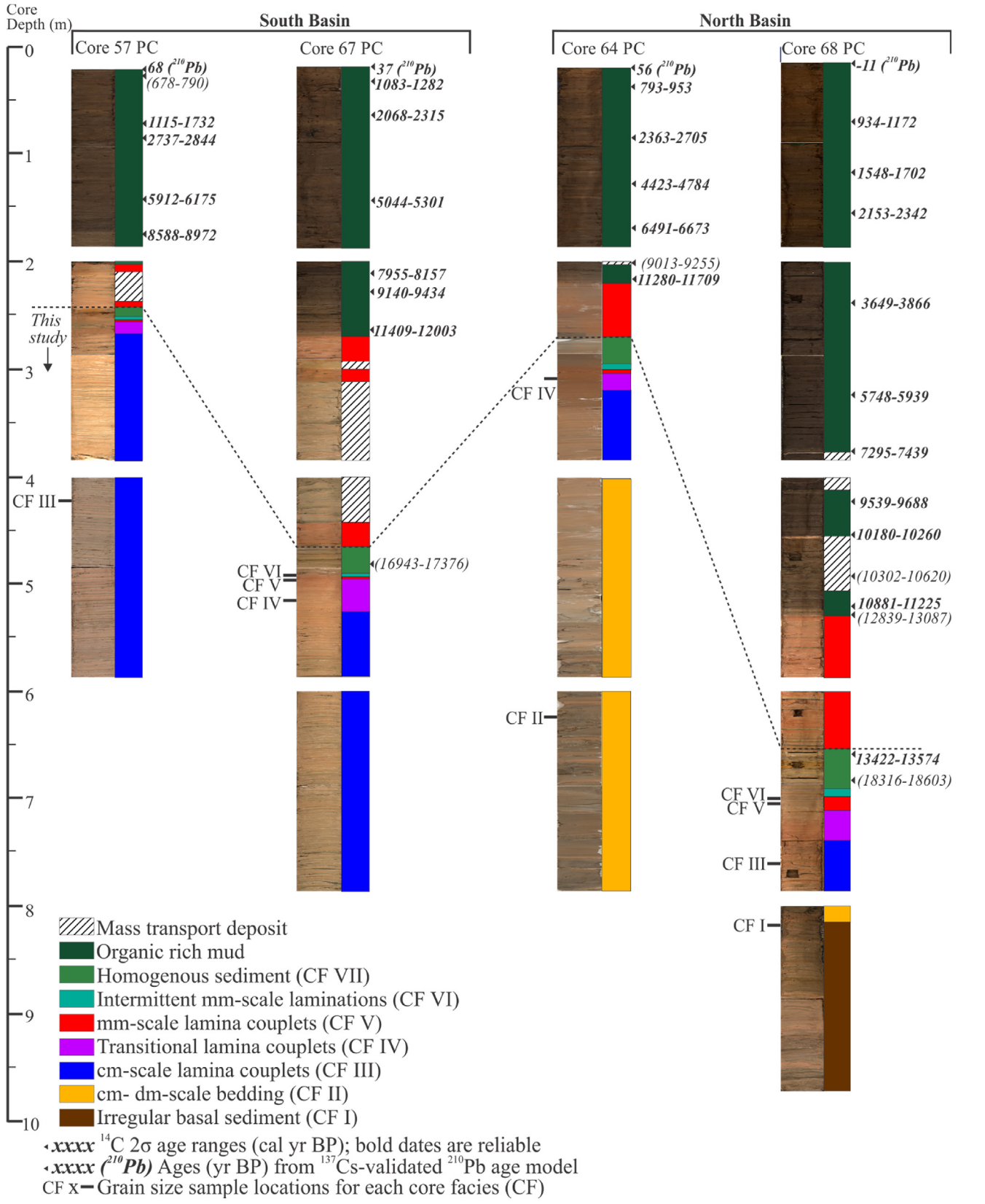

Fig. 5. Stratigraphy of the four studied cores in Windermere. For each core, a split-core photograph is shown (left), along with a colour-coded log showing the locations of the sediment types. 2-sigma radiocarbon date ranges are shown to the right of each core in cal yr BP, and unreliable dates (or dates from mass transport deposits) are shown in brackets (see text for discussion). Dates at the top of each piston core from a 137Cs-validated 210 Pb age model are also shown. The locations for grain size samples for each core facies (CF) are shown to the left of each core. Sediments forming the focus of this paper are below the dotted line. (For interpretation of the references to colour in this figure legend, the reader is referred to the Web version of this article.)

sedimentation (boundary between CF-V and CF-VI in Fig. 5) corresponds to the onset of the Lateglacial Interstadial (~14.7 cal ka BP), then our radiocarbon dates from the lower interstadial unit are 2000–4000 years too old. These seem large, but reservoir age corrections of up to 3260 yr have been documented in Tibetan lakes (Wu et al., 2010). Although a soft-water lake throughout the Holocene, the early-interstadial Windermere may also have been subject to a 'hardwater effect' (Pennington, 1977), since there was significant calcite and dolomite found in the basal sediment and thicker cm-scale laminations deposited in the lake (see section 5.4) that could also have contributed to an anomalously old age for the lake's dissolved inorganic carbon reservoir (Philippsen, 2013). These excessively old dates are consistent with the age of 17.8 ± 0.9 ka obtained from Low Wray Bay, Windermere at a similar stratigraphic position by Coope and Pennington (1977). In agreement with other researchers' conclusions that Coope and Pennington's (1977) ice-free date of 17.7 cal ka BP is aberrant or of poor data quality (Small et al., 2017b; Tipping, 1991; Wilson et al., 2013; Wilson and Lord, 2014), we consider our unusually old Lateglacial Interstadial dates to be similarly inaccurate.

Taking CF VI and CF VII (Fig. 5) as the Lateglacial Interstadial, pre-interstadial sediment did not contain enough carbon to perform radiocarbon dating (and it would probably have been subject to old-carbon in wash in any case). Additionally, no tephra layers were found. This section of the archive therefore relies on our interpreted varve chronology, which should be considered floating, but immediately before the onset of the Lateglacial Interstadial. On the GICC05 (Greenland ice core) timescale, the start of the Lateglacial Interstadial (GI-1) occurred at 14,642 ± 4 yr BP (Rasmussen et al., 2014). Synchroneity of Lateglacial climate events cannot be assumed between Greenland and north-west Europe but since remains of the temperate-dwelling species *ursus arctos* (brown bear), ^{14}C-dated to 14.8–14.7cal ka BP, have been found in caves in the Pennines south-east of the Lake District (Lord et al., 2007; O'Connor and Lord, 2013), it is reasonable to use ~14.7 ka BP to mark the onset of the Lateglacial Interstadial in northwest England.

5.3. Pre-Younger Dryas sediment facies

Core stratigraphy and available dates indicate that Windermere deglaciated prior to the Lateglacial Interstadial. We focus our study on the deglacial and immediately post-glacial development of the basins, and describe here the sediment facies up to and including the Lateglacial. Seven sediment types are present in the pre-Younger Dryas parts of the studied cores (Fig. 6) are, from core bottom to top, as follows: disturbed basal sediment (Core 68 only); centimetre to decimetre-scale beds (Cores 64 and 68 only); centimetre-scale beds; thinning transitional laminations; millimetre-scale laminations; indistinct and intermittent laminae; and homogenous sediment. Each sediment type has been assigned a 'Core Facies' (CF) from I to VII. A summary of the different sediment types is given in Fig. 6, and sediment descriptions, as well as the corresponding seismic facies of Pinson et al. (2013), are given in Table 2.

5.4. Geochemistry and mineralogy

EDS maps were produced to identify major constituent minerals in the cores, complemented by XRD analysis. The main silt- and sand-sized minerals identified in the XRD study of the base of Core 68 (~8.8 m) are quartz, plagioclase feldspar, orthoclase feldspar, and calcite (Table 3). EDS mapping of this sediment also identified a single grain of Fe_2O_3, as well as dolomite, apatite, and rutile (Fig. 7).

EDS mapping of selected sediment from the cm-scale beds of Cores 57 and 67 also indicate the presence of quartz, dolomite, rutile, apatite, and ferric oxide (Fig. 7). Much of the sediment is made up of indistinguishable oxides of Si, Al, Mg, Na, K, and Fe in varying proportions, indicating possibly clinochlore and feldspars. Occasional Cu-rich grains are present.

A major compositional change is shown with calcium (Ca) in both Itrax XRF curves (Fig. 8) and in EDS phase maps (Fig. 7). In the cm-scale beds and outwash sediments, calcium levels are high, and EDS phase maps show that the constituent Ca-bearing minerals are calcite, dolomite, and fluorapatite. As the beds thin to mm-scale couplets, the amplitude of the Itrax calcium signal decreases and the EDS phase maps show that the calcite and dolomite are lost. Ca content then remains minimal for the remainder of the core sequence and only a small amount of fluorapatite contributes any calcium to the silt layers. (Fig. 8).

5.5. Grain size

Grain size modes for each sediment type and for each basin (Fig. 9) are summarised in Supplementary Table 2. Note that from estimates of grain size in BSEI there are modes in the different facies that are not always found in the modes given by the Laser diffraction analysis, however, the general characteristics may be observed. Grain size classifications are those given in Blott and Pye (2001) and Friedman and Sanders (1978). There is a general trend of decreasing grain size primary mode from CF I – CF V (from ~16 to 2–4 μm), and the North Basin samples also tend to have higher modes than those of the South Basin by up to 4 μm.

6. Facies interpretation and significance

We now place the different Core Facies (CF) in an interpretative context related to the progressive deglaciation of the Windermere catchment.

6.1. Basal sediments (CF I) and cm – dm beds (CF II): lake-terminating ice margin

The basal sediments in Core 68 (Core Facies (CF) 1, CF II; Table 2), the northernmost core, are interpreted to represent ice-proximal deposits influenced by a chaotic ice-marginal glaciofluvial regime, and represent the highest-energy sedimentary environment of the core suite. In combination with stratigraphic position, lack of any organics, and local glacio-geomorphology, this is supported by the alternation of well-sorted silt and sand beds (Fig. 6k; Fig. 7c); presence of massive sand beds including some more poorly sorted beds of medium sand grade with coarse sand grains in the basal 50 cm of Core 68; and evidence of soft-sediment deformation including convolution and fluid escape structures. The cm-dm-scale beds present in Cores 64 and 68 of the North Basin (CF II) are interpreted to be ice-proximal based on bed thickness and grain size (Fig. 9), but, although some disturbances are present, are much less chaotic. These beds are most likely varves, based on their apparent regularity and similarity to varves up to ~20 cm thick found in North America (Ridge et al., 2012); ice-proximal varves 20–75 cm thick have also been reported from southern Sweden (Ringberg, 1991). The silt melt-season layer is between 9 and 30 cm, but the clay winter layer is only 0.4–2 cm. This proportionally thicker summer layer, with grains as coarse as very fine sand, indicates close proximity of the site to the mouths of subglacial water outlets, sediment transport by underflows, and possibly rapid melting (Ringberg, 1991). The Core 64 CF II cm-to dm-beds, that we interpret as probable varves, were likely deposited very soon after ice recession (Björck and Wohlfarth, 2001; Ridge et al., 2012; Wohlfarth et al., 1994).

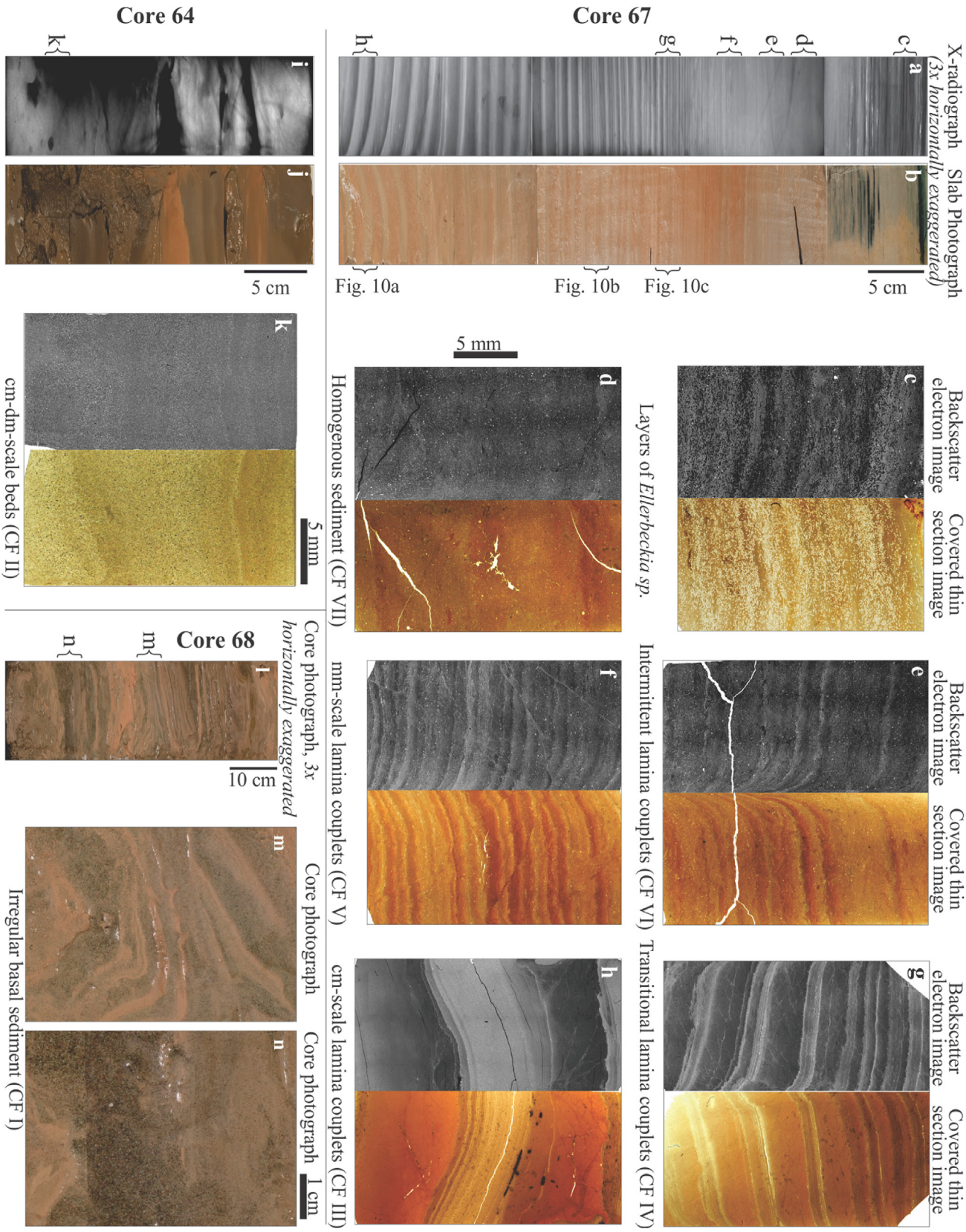

Fig. 6. Summary of major sediment types. a) X-radiographs of Core 67; b) slab photographs of Core 67; c) Backscatter electron image (BSEI) and thin section image (TSI) showing layers of *Ellerbeckia* sp.; d) BSEI and TSI of full Interstadial sediment; e) BSEI and TSI of intermittent lamina couplets; f) BSEI and TSI of mm-scale lamina couplets; g) BSEI and TSI of thinning transitional lamina couplets; h) BSEI and TSI of cm-scale lamina couplets; i) X-radiograph from Core 64; j) Slab photograph of Core 64; k) BSEI and TSI of cm-dm-scale beds; l) Split core photograph from Core 68; m) split-core photograph of disturbed basal sediments; n) split-core photograph of disturbed basal sediments.

Table 2
Descriptions of the seven main sediment types (core facies; CF) present in the cores, stratigraphically from top to bottom. Sediment type stratigraphy may be seen in Fig. 5, and references to images of the various core facies in Fig. 6 are given in the second column. The core facies are also related to the seismic facies of Pinson et al. (2013).

Sediment Type	Core Facies	Seismic facies	Description
Homogenous Sediment *All four cores*	CF VII (Fig. 6a, b, c, d)	IIa in North Basin, IIb in South Basin	A relatively homogenous silty clay with fairly homogenously-distributed coarse to very coarse silt clasts and numerous microfossils, some plant fragments, and indeterminate organic particles present. Core 68 contains cm-scale variations in colour and density, with diagenetic iron-rich greigite (Fe_3S_4) (Supplementary Fig. 2). Several ~1–2 mm thick laminations of the freshwater tychopelagic diatom genus *Ellerbeckia* sp., are present in Core 67 (Supplementary Fig. 2). The diatom layers have higher concentrations of coarse detrital grains.
Intermittent indistinct laminae *All four cores*	CF VI (Fig. 6a, b, e)	IIa in North Basin, IIb in South Basin	2–5 mm thick transitional bundles of intermittent, indistinct laminae comprising very fine to medium silt, with coarse and very coarse silt grains dispersed homogenously throughout. CF VI is similar to a mm-scale lamina, but instead of a pure clay cap, the sediment is more a silty clay containing several microfossils including testate amoebae, chironomid and diatom fragments, lithic larva cases, or moulds left by decayed organisms. These laminae become more intermittent into CF VII up-core.
Millimetre-scale lamina couplets *All four cores*	CF V (Fig. 6a, b, f)	IIa in North Basin, IIb in South Basin	The bases of the millimetre-scale laminae typically comprise medium silt grading to fine silt that may contain trains of medium silt and isolated coarse silt grains. The clay cap exhibits small fluid-escape and bioturbative structures at the top of the silt layer, which may make the upper and lower boundaries of the clay cap harder to distinguish.
Transitional thinning cm-mm lamina couplets *All four cores*	CF IV (Fig. 6a, b, g)	IIa in North Basin, IIb in South Basin	The grain size is very fine silt in the South Basin but the North Basin also contains a medium to very coarse silt fraction. These couplets, which thin up-core from ~1 cm to ~1 mm, are distinguished by the presence of multiple internal silt sublaminae and sub-laminae richer in clay ~0.1–1 mm-thick.
Centimetre-scale lamina couplets *All four cores*	CF III (Fig. 6a, b, h; Fig. 4)	IIa in North Basin, IIb in South Basin	A well-defined ~0.8–~6 cm thick couplet comprising a fine to very fine silt layer overlain by a clay layer. The silt component often comprises several discrete silt sublaminae of 0.5 mm–2 mm, which may contain very coarse silt to very fine sand grains (rare in the South Basin). The well-defined clay cap is usually at least as thick as the silt layer, and often exhibits vein structures similar to those attributed to palaeoseismicity (Brothers et al., 1996). Occasionally a very thin (single-grain) silt layer or train of silt grains interrupts the clay cap. The clay-silt contact at the base of the overlying bed is very sharp, and micro- load casting is common.
Centimetre to decimetre-scale bedding *North Basin only*	CF II (Fig. 6i, j, k)	IIa (possibly transitioning to I)	The beds largely comprise multiple ~0.1 mm to ~1 cm bands of well-sorted medium to very coarse silts and very fine sand, with a clay cap. The bed thickness ranges from ~31 cm at the base of Core 64 (~7–8 m) to only ~2 cm at ~4 m depth, while in Core 68, the layers are only a maximum of ~13 cm thick.
Irregular basal sediments *Northernmost core (68) only*	CF I (Fig. 6l, m, n)	IIa (possibly transitioning to I)	Thin bedded silts and clays with thin beds of fine to very fine sand increasingly common to the base. Fluid escape structures, convolution, folding, and micro-faulting are common. Coarse sand occurs at > 9.5 m depth. The finer sediment is well-sorted, but beds containing coarse grains are poorly sorted.

Table 3
X-ray diffraction results from a sediment sample from the base of Core 68, situated ~2.5 m above the base of SF IIa.

Mineral	%
Plagioclase Feldspar	18.1
Calcite	3.8
Chlorite (clay)	6
Orthoclase (K) Feldspar	3.9
Quartz	48.3
Illite (clay)	20
Total Clay	26
TOTAL	*100*

6.2. The lamina couplets of CF III to CF V- a varve interpretation

The centimetre-scale to millimetre-scale lamina couplets of CF III to CF V (Table 2) are interpreted as varves based on their sedimentary characteristics. Lamina couplets defined as varves have a component characterised by a simple or composite (sublaminated) unit of coarser material, typically silt, interpreted as a melt-season layer. This coarser unit is capped with clay, taken to be the non-melt season component formed by the slow settling of fines through the water column. The regularity of these lamina couplets, and the presence of the clay cap with characteristic sharp contact with the overlying silt, forms the first basis for a varve interpretation. The close resemblance of the Windermere lamina couplets to examples of proven varves from Alpine (Amann et al., 2014), High Arctic (Chutko and Lamoureux, 2008; Kaufman et al., 2011), and montane Canadian (Menounos and Clague, 2008) settings provides additional support for our varve interpretation. A further approach to validate the annual occurrence of laminations is the demonstration of lateral consistency in different cores from the same lake (Zolitschka et al., 2015) and we report the close match between Cores 57 and 67, some 2.25 km apart, in section 7, below.

6.3. CF III: cm-scale varves-less proximal ice margin

The cm-scale thickness of the cm-scale CF III varves, and the common presence of complex melt-season layers containing multiple micrograded units or sublaminae (Fig. 4; Fig. 6h; Fig. 10), are both fundamental characteristics of glacial varves (Blass et al., 2003; Ridge et al., 2012) indicative of a proglacial lake setting at the time of their formation. Distinct sublaminae at the base of the varve represent early-season melt and run-off (Fig. 6h), whilst micrograded sublaminae within the main melt season sediment

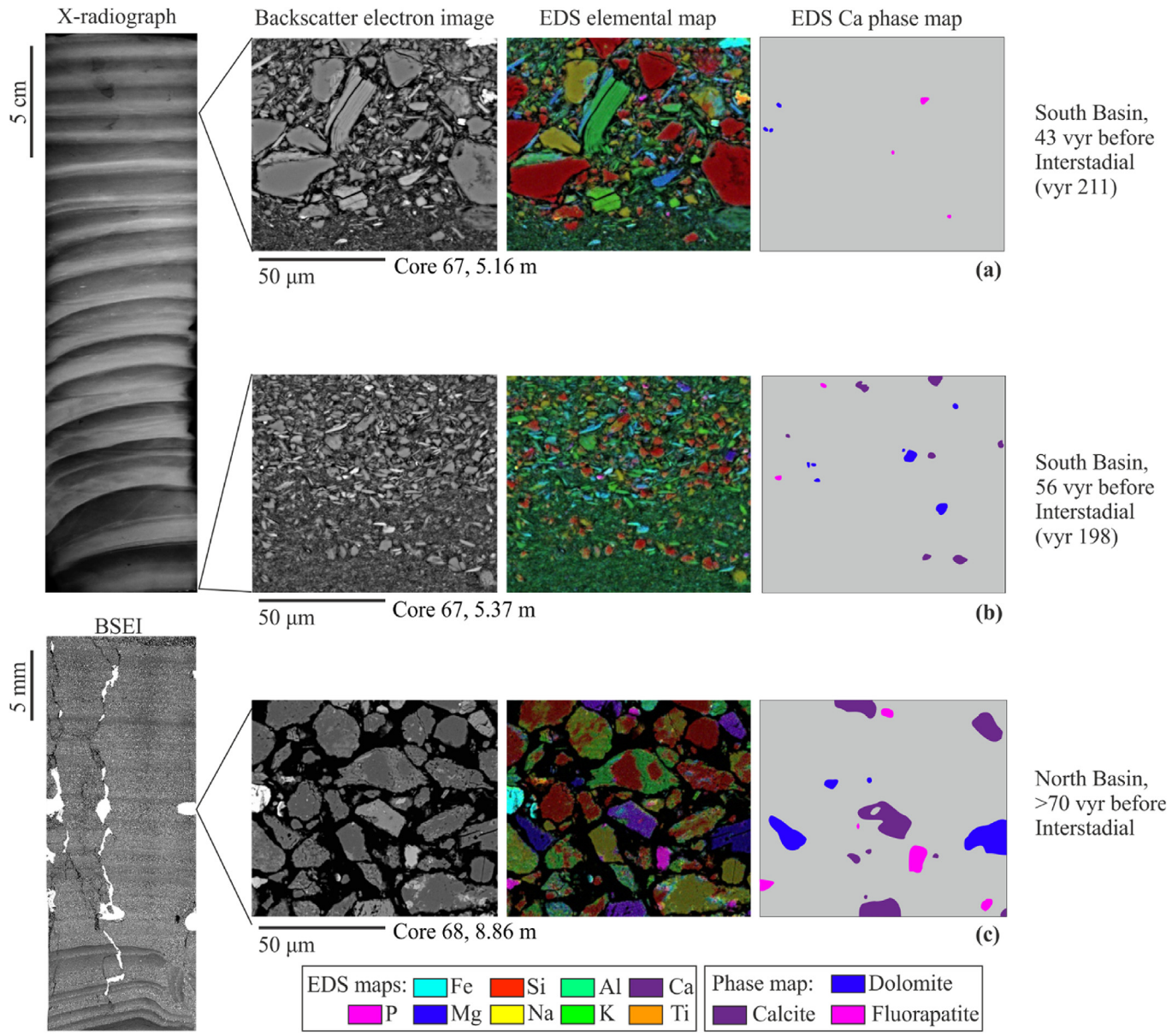

Fig. 7. Energy-dispersive X-ray spectroscopy (EDS) maps demonstrating the differing calcium content upcore. Far left: X-radiograph (top panel) or BSEI (bottom panel) showing the sediment overview. Left: BSEI of sediment. Middle: EDS elemental map showing the elements present. Right: EDS mineral phase map showing which calcium-bearing minerals are present. Far right: Lake basin and timeframe. (a): basal coarser silt layer resting above clay from CF IV (Transitional thinning lamina couplets) (b) basal, very fine silt resting on clay from CF III (cm-scale lamina couplets). (c): Coarse silts from the basal sediments of the North Basin – CF I.

represents discrete ice melt events over the summer (Blass et al., 2003; Ridge et al., 2012). Separate silt sublaminae within the clay cap, where present, likely represent late-season melt events. The fine grain size of the South Basin melt-season layers (median ~2.9–3.2 μm, mode 3.82 μm; Fig. 9; Fig. 7b) is evidence of deposition from suspension without a bedload component (Gammon et al., 2017). This indicates that either the varves were formed ice-distally, the absent coarser fraction having been deposited more proximally to the ice margin (cf. Smith et al., 2004; Zolitschka, 1996); or that the coarse fraction was trapped by lakebed topography such as the moraine ridges or the basin-separating sill (Fig. 1; Fig. 2a). In contrast to the South Basin CF III varves, those of the North Basin contain appreciable medium and coarse silt fractions and isolated sand grains (Fig. 9) representing underflow transport, and closer proximity of the glacier to the lake.

6.4. CF IV: transitional, thinning cm to mm-scale varves- ice retreats along the catchment valleys with increasing nival and pluvial seasonal input

The varves of CF IV have a similar structure to those of CF III, with complex melt-season layers, but they are mostly thinner and the micrograded sublaminae grade more abruptly to very fine silt and clay (Fig. 6g; Fig. 10). In the South Basin cores, the thickness of the main melt season very fine silt layer decreases up-core and it is replaced by multiple, thin (50–500 μm) sublaminae of fine to medium silt and occasionally coarse silt and very fine sand (Fig. 7a). The reduction in overall varve thickness as well as that of the main melt season silt suggests decreasing influence of glacial meltwater (cf. Palmer et al., 2008), while the multiple sublaminae of varying thickness and grain size suggest sediment delivery by more diverse

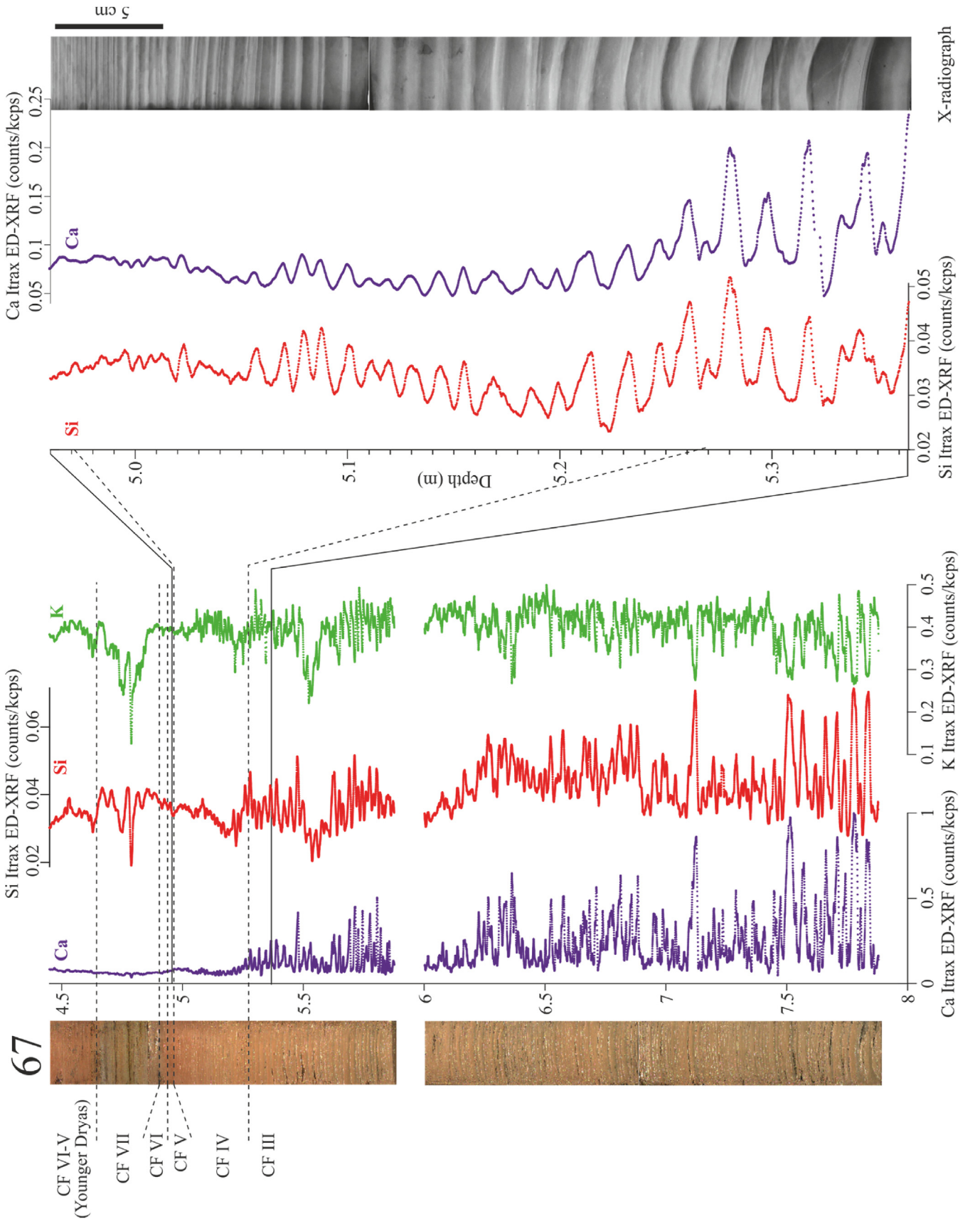

Fig. 8. Elemental variation in Core 67 derived from Itrax data (20-point smoothed profile) at different scales upcore from the core base to the onset of Younger Dryas-age mm-scale lamina couplets. Left: Core photo of Core 67 with Itrax variations in calcium (weathering and ice transport indicator), silica (lamina coarse component indicator), and potassium (lamina clay component indicator). Right: Expanded section with silica (coarse component indicator) and calcium (ice transport indicator) through the transition from cm-scale lamina couplets to mm-scale lamina couplets, augmented by an X-radiograph negative of the section. Boundaries between sediment types (CF I – VII, see Table 2) are shown as dashed lines.

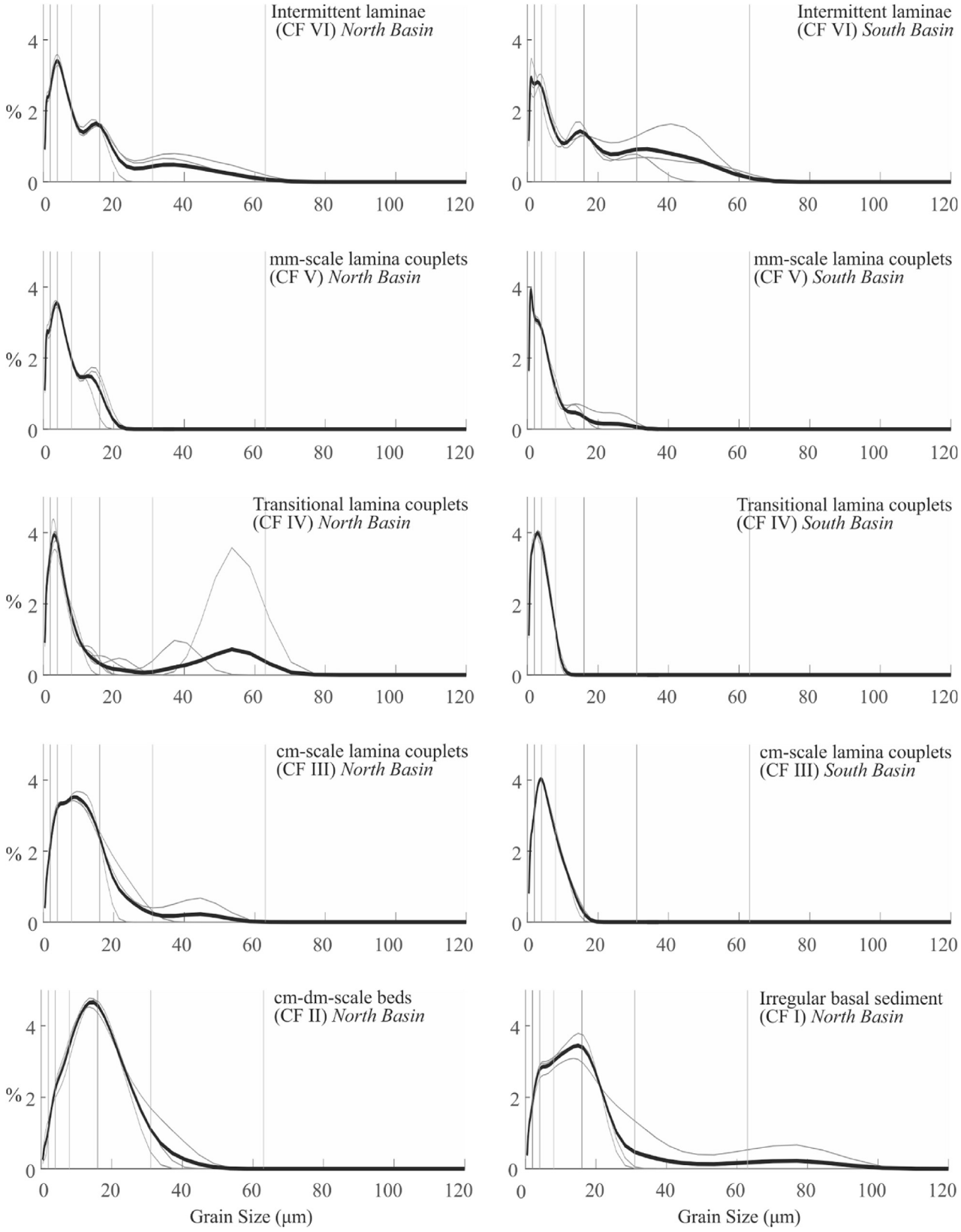

Fig. 9. Grain size distributions for samples of each sediment type. Thin grey lines are the individual subsamples from the same powdered sample, and the thicker black line shows the mean for these subsamples. Vertical lines are the lower grain size boundaries as follows: Blue- Very fine silt (2–4 μm); Orange- Fine silt (4–8 μm); Yellow- Medium silt (8–16 μm); Purple- Coarse silt (16–31 μm); Green- Very coarse silt (31–63 μm); Blue- Very fine sand (63–125 μm). Grain size classifications are those given in Blott and Pye (2001) and Friedman and Sanders (1978). Stratigraphic locations of samples are given in Fig. 5.

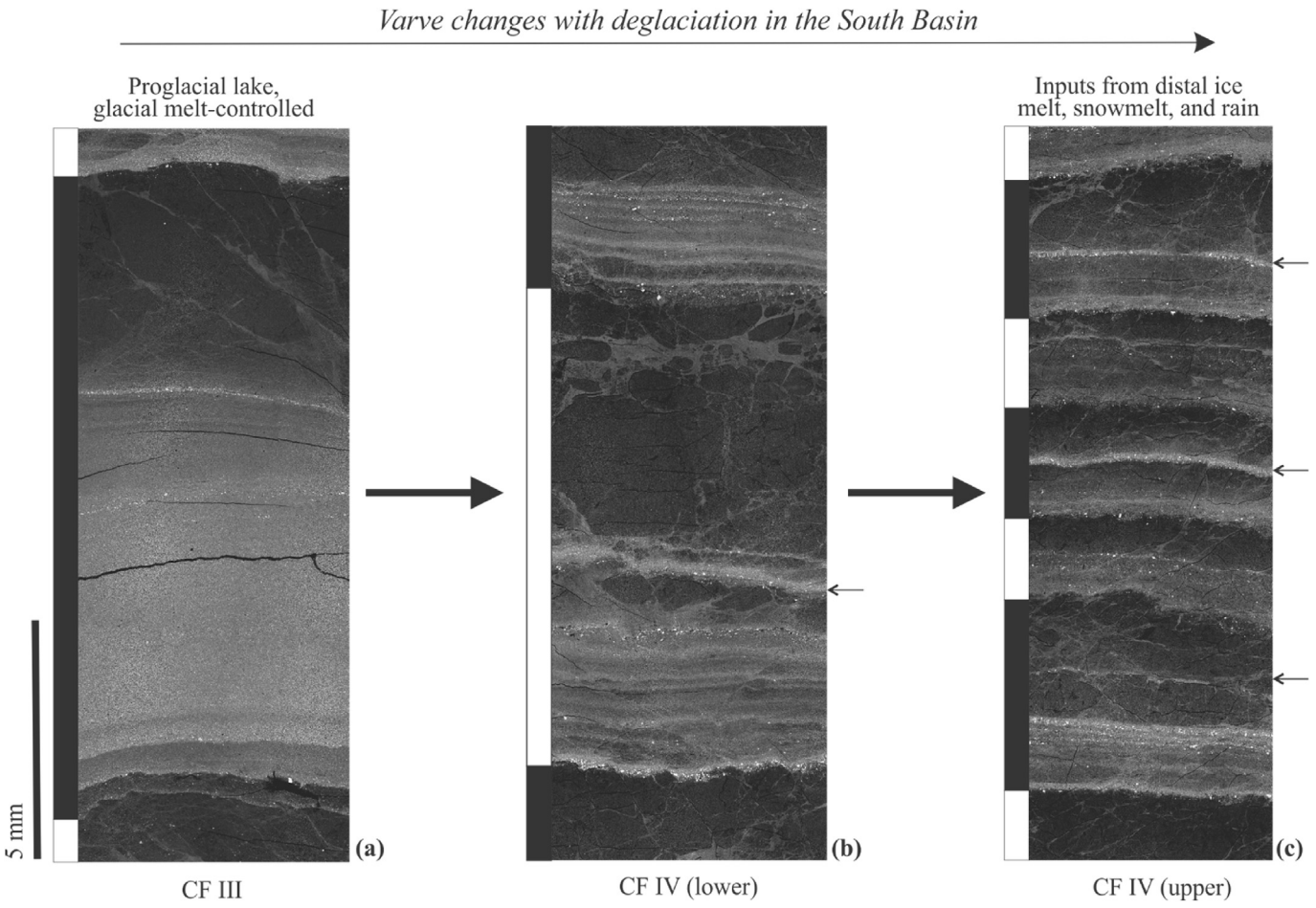

Fig. 10. Backscatter electron images showing changes through deglaciation from Core 67 (locations shown on Fig. 6a). Varves are indicated by the black and white bars to the left of each panel. The left panel shows the cm-scale varves of CF III. The mid and right panels show the transitional varves of CF IV thinning from cm-scale (mid panel) to the mm-scale (right panel) with multiple silt sub-laminae. Isolated sublaminae in the clay upper section of the varves, indicated by small arrows to the right, are likely runoff from late summer/autumn storms (see text for further discussion).

hydrologic processes. The multiple sublaminae closely resemble those occurring in catchments where glacier margins are remote from lakes, and where summer snow melt and summer and autumn rainfall events are also important delivery mechanisms such as those documented in British Columbia by Menounos and Clague (2008) and Cockburn and Lamoureux (2007). In the upper, thinning, varves of CF IV, more medium to coarse silt grains occur, often as sublaminae within the clay upper section of the varve (Fig. 10) that resemble similar features attributed to runoff from late summer/autumn rainstorms (cf. Moore et al., 2001; Smith et al., 2004).

6.5. CF V: mm-scale varves-largely ice-free catchment with dominant snowmelt influence

The thinner millimetre-scale varves of CF V are characterised by a reduced melt-season layer complexity (Fig. 6f; Fig. 10) and continuance of fine grain size primary modes (1, 3–4 μm; Fig. 9), but also contain a medium silt component and are closely comparable with snowmelt-derived varves from Arctic Canada and Alaska (Francus et al., 2008; Hughen et al., 1996). The increase in coarse grain size fractions in the south Basin indicate direct runoff. We infer that the Windermere catchment was mostly ice-free when these varves formed. Varves ~1 mm thick are known to have formed in Windermere during the Younger Dryas (Avery, 2017; Pennington, 1943) when the catchment was minimally glaciated (Brown, 2009; McDougall, 2001; Sissons, 1980; Wilson, 2004; Wilson and Clark, 1998), and we expect that the pre-Interstadial CF V varves had similar source conditions. Intermittent evidence of bioturbation and microfossils in CF V is indicative of organic production in the lake and associated activity of benthic organisms, also evidencing environmental amelioration at this time. We take the first mm-scale varve that exhibits significant evidence of scattered coarse clasts, microfossils, and bioturbation, to mark the nominal onset of the warm Lateglacial Interstadial (see Fig. 11).

6.6. Post-varve sediments (CF VI and CF VII): The Lateglacial Interstadial- organic deposition and intermittent flood input

The increased porosity in backscatter electron images (Fig. 6) and the presence of amorphous organic matter and microfossils including testate amoebae, diatoms, chironomids, and seeds, indicates productivity in the lake within a catchment that was vegetated with developing soils. The now-regular presence of coarse silt grains throughout the intermittent lamina matrix and the presence of grain populations around 40 μm in both basins (Fig. 9) indicates a sediment source other than dwindling glacionival melt. It is likely that this coarser fraction entered the lake through floods and runoff from a deglaciated landscape resulting in

a higher runoff intensity. The increased intermittency of the laminae likely reflects decreased recurrence of years with sufficient snow to produce significant runoff, together with increased benthic activity. CF VII is the deep-water equivalent of Pennington's 'grey layer' (Pennington, 1943), containing myriad micro- and macrofossils, which eventually became the defining sediment of the Lateglacial 'Windermere' Interstadial in Britain (Coope and Pennington, 1977).

Whilst the shallow-water sediments of Low Wray Bay contained distinct sedimentary (and indeed palynological and entomological) phases, Pennington's deep-water interstadial sediments sometimes only showed a brief cessation of varves (Coope and Pennington, 1977; Pennington, 1947). Although we have not focused on the interstadial sediments in detail, we note that in the interstadial sediments of Core 67, ~1 mm thick laminae containing monospecific concentrations of *Ellerbeckia* sp. (Fig. 6c; Supplementary Figs. 2a–c) are also accompanied by a higher concentration of coarse silt grains, suggesting that these may represent intense runoff events from the Cunsey Beck valley (Fig. 1) that washed in this benthic, shallow water diatom to deeper parts of the lake. In the interstadial sediments of Core 68, there are cm-scale bands of more- and less-dense sediment, and particularly in the middle of the unit there are growths of greigite (Fe_3S_4; Supplementary Figs. 2d–e). These growths also appear to a much lesser extent in the interstadial sediments of Core 57, and indicate anoxic, sulphate-reducing conditions in the deeper basins during the Lateglacial Interstadial (Roberts et al., 2011 and references therein). Similar growths from the early Lateglacial Interstadial from Hawes Water, northwest England, are interpreted to have formed due to warmth-induced organic productivity (Nolan et al., 1999; Oldfield, 2013).

Above this unit (CF VII), all the cores contain Younger Dryas-age laminated sediments including some mass transport deposits, and above that are Holocene muds and gyttja (Fig. 5).

7. Varve sequences and varve correlation between cores

Core Facies III-V are varved, and we have produced varve thickness measurements for these facies (Avery et al., 2019). The total number of varves in each sequence, along with counting uncertainties (see methods), is given in Table 4 below. Supplementary Fig. 4 shows varve number information on stratigraphic core diagrams.

In order to derive a composite chronology for deglacial varve sedimentation in Windermere, cores are correlated by drawing on distinctive marker beds and trends in varve thickness, mineralogy and geochemistry. A match between the varve thickness sequences of South Basin Cores 57 and 67, anchored by 16 well-correlated reference varves, is unequivocal (Fig. 11). The varve thickness records for Cores 57 and 67 have accordingly been placed on the same numerical scale. The Core 57–67 component of the 'master' chronology constitutes a combined 273 varve years. The varve that marks the nominal onset of the Lateglacial Interstadial (containing microfossils, bioturbation, and increased organic content) is varve 254 on this master chronology.

The general thickness trend of CF III varve thicknesses in Core 64 appears to broadly agree with that of the South Basin, although individual year thicknesses are not the same. The first eleven varve thicknesses after the mass transport deposit (MTD) in Core 64 also match well with those of Core 67, and formed part of the basis for the MTD duration. According to our correlation, the onset of the similar general thickness trend occurs 183 vyr after the lowermost varve recovered from the South Basin. Since the correlations with Core 64 are based only on thicknesses and not on marker varves (the sediment type differences between the basins prevent this), we still show the Core 64 record on its own numerical scale in Fig. 11. The thicker (up to 314 mm) CF II varve thicknesses in the lowermost part of Core 64 do not display any similarity to the South Basin varve thicknesses. These varves would have formed in a locally-controlled environment near the ice-margin, and their thicknesses would be unlikely to correlate with other locations (Holmquist and Wohlfarth, 1998).

The thickness measurements for Core 68 appear very different from those of the other cores, with e.g. 96 CF IV varves (as opposed to 36 in the South Basin cores), none of which look visually similar to any possible marker varves in the other cores. Therefore it was not possible to tie the Core 68 varve chronology to that of the South Basin (Fig. 11) using varve thicknesses, and the Core 68 chronology forms a second floating part of the overall chronology.

A distinctive change in mineralogy and geochemistry, likely marking a shift in sediment provenance, may also be used to aid correlation between cores. As can be seen in Figs. 7 and 8, the marked reduction in levels of Ca in the Itrax measurements occurs alongside the disappearance of calcite and dolomite limestone fragments in the sediment. The most likely origin of the limestone fragments is from the Dent Group (formerly Coniston Limestone) running discontinuously west-east across the northernmost part of the modern lake, along with some other calcareous formations in the Windermere Supergroup farther south. The Dent group is the northernmost significantly-calcareous group or formation in the Windermere catchment (formed in shallow lime mud seas 444–449 Ma immediately after the Ordovician volcanism that formed the Lake District uplands), and contains both calcitic and dolomitic limestone (McNamara, 1979; Mosely, 1984). The lack of effervescence in the tills collected farther north of the group supports this interpretation.

The Ca Itrax signal is a distinct marker suggesting a change in sediment input to the basins at this interval. Given that the main ice masses, and therefore sediment sources, lay to the north of the lake, we assume that the Itrax Ca signal in Core 68 (the northernmost core) is unlikely to have reduced before that of the other cores, and that the onset of CF IV and CF V also did not occur in Core 68 before the other cores. We therefore use the cessation of the Ca signal as a tiepoint for an 'earliest-possible' placement of the Core 68 varve chronology onto the master varve chronology (Fig. 11). In this case, varve 18 from Core 68 would translate to varve 209 of the master chronology; the tiepoint is followed by a further 203 varves at site 68, until the onset of CF VI during the beginning of the Lateglacial Interstadial. This effectively extends the master chronology to 412 vyr, although it could potentially be longer if the true placement in Core 68 is later.

8. Deglacial history

The succession of facies and varve thicknesses in the Windermere cores (Figs. 5 and 6) shows a transition from a glaciated catchment with a valley glacier terminating towards the southern end of the North Basin (CF I-III), to an unglaciated vegetated catchment (CF VI-VII) at the onset of the Lateglacial Interstadial. The varve sequences are used in this way to understand better the nature and timing of the retreat of the ice in the catchment and the wider implications.

8.1. Ice retreat along the lake basins of Windermere

Seven buried recessional moraines (RMs) identified in the subsurface seismic profiling data indicate that ice actively retreated north along the South Basin of the steep-sided Windermere Valley and was marked by several still-stands or small readvances, although no constraining ages are currently available (Fig. 2; Fig. 3;

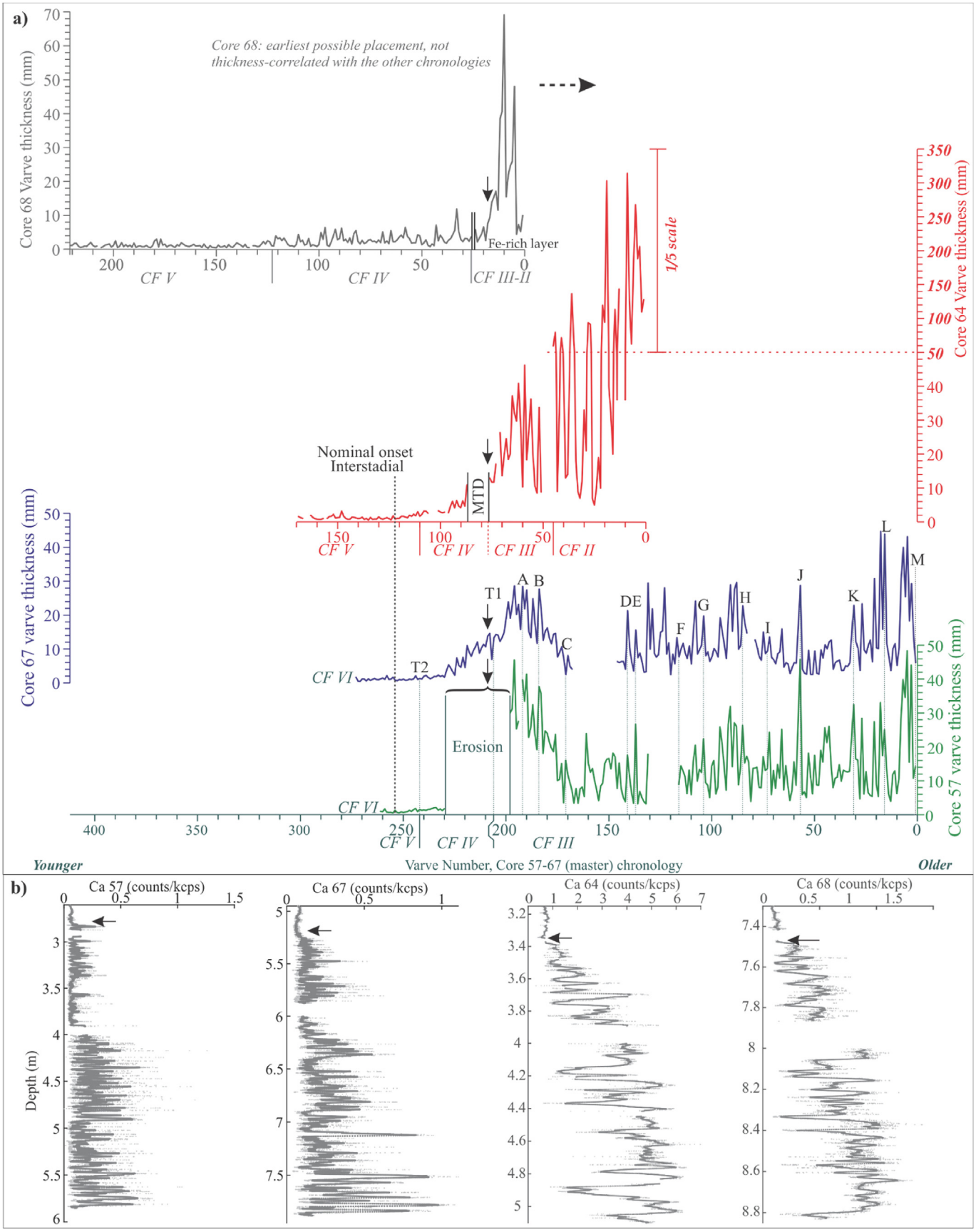

Fig. 11. a) Pre-Interstadial varve thickness sequences in millimetres. Core 68 (grey), Core 64 (red), Core 67 (blue), and Core 57 (green), placed on local chronologies. Note that the vertical scale for Core 64 is compressed above 50 mm for space reasons. Vertical black arrows indicate the where the Ca signal diminishes in the Itrax data, representing the

Table 4
Summary of pre-Interstadial varve counts.

Core	57	67	64	68
No. varves CF V	20	32 [+1–2]	60 [-4]	100 [+3-3]
No. varves CF IV	12 (24 missing)	36	23 (+up to 9 eroded by MTD below)	96 [+2-2]
No. varves CF III	183 (7 missing) [+1]	181 [+2]	27 [+2]	25 [+3]
No. varves CF II	0	0	43 (+maybe 7 in core gaps) [+3–1]	0
No. varves Total	215 [+1]	249 [+3–2]	153 (+~14 eroded or core gap: 167) [-5 +5]	221 [+8–5]
Error (%)	0.47	2.01	5.99–6.54	5.88
No. varves 57–67 combined	261	273		

Pinson et al., 2013). The series of tills and moraines that demonstrate the ice retreat (SF I; Table 1, Fig. 2), are overlain by seismic facies SF IIa and SF IIb, which have parallel layered internal reflections and are interpreted as glaciolacustrine sediments. SF IIb constitutes the cm-scale varve facies (CF III) penetrated by Cores 57 and 67. We note that South Basin cores did not bottom in basal glacial sediments.

The fine grain size of the SF IIb/CF III varves (very fine silt and clay) attests to settling from suspension (Gammon et al., 2017), and, together with the close correlation of varves between Cores 57 and 67 (some 2.25 km apart), is consistent with deposition from meltwater plumes from a distal ice margin. These meltwater plumes were likely sourced from a glacier whose margin lay to the north of the bedrock high between the basins (now represented by a series of islands including Belle Isle; Fig. 1) which acted to block any bed load and coarser suspended load size fractions from reaching the South Basin at this time. This interpretation is consistent with that of Pinson et al. (2013), who hypothesised that the transition in seismic facies from SF IIa to SF IIb in the South Basin represented a change due to bedrock highs between the sub-basins, which limited sediment southward transport to suspended load delivered by overflow as the ice margin retreated northwards. The excellent correlation between the varve thicknesses of Cores 57 and 67, 2.25 km apart, suggests that sediment trapping by the bedrock high caused a uniform sedimentary response in the South Basin to glacier melt, independent of margin proximity. We also note that the continuous presence of the varves in the South Basin shows that the two lake basins were connected at this time, and that the lake level cannot have been more than 4 m lower than the lake's modern level (the depth of the sill between the basins).

The northward retreat of the ice along the North Basin is recorded by two recessional moraines and 28 DGMs and potentially more between RMs 8–9 where gas blanking precluded seismic reflection imaging (Pinson et al., 2013, Figs. 2 and 3). De Geer moraines are considered to represent short-term still-stands in the ice margin position (Bouvier et al., 2015), usually occurring in regularly spaced sequences indicating rhythmic retreat. Our varve sequence correlation shows that the formation of varves at site 64 was already underway at around varve 133 on the master chronology. The coarse grain size and large thickness of the silt layer suggests that the bottom varve may have been deposited not long before (although with up to 5 m CF I sediment below this), that the glacier terminus was likely very proximal, and that it may have been undergoing rapid retreat. The coarseness and thickness of the summer layer additionally provides evidence of significant drainage of the Troutbeck valley glacier at this time (Fig. 1). The sediment-trapping ability of the sill between the basins is also demonstrated, with the South Basin receiving fine sediment in summer from overflows and the North Basin receiving the coarse sediment by underflows.

The onset of CF III varves in Core 64 at varve year 183 on the master chronology coincides with a varve thickness increase in the South Basin, suggesting that as the glacier retreated northwards, there was an increase in meltwater-borne suspended sediment load transport across the bedrock high between the basins. The earliest-possible placement of the Core 68 varve record starts at varve 192 on the master chronology. There are many layers below this that may also be varves in addition to ~2.5 m CF I sediment below core penetration, providing evidence that the glacier terminus was well north of site 68 by varve 183. We suggest that the onset of CF III varves in the North Basin, along with the thickness increase in the South Basin, may have occurred when the glacier retreated out of the North Basin and into what is now the lowland terrestrial valley just north of the lake. The increase in fine material may be due to lake-proximal meltwater streams transporting loose, glacially-eroded sediment situated immediately to the north of the proglacial lake as the glacier retreated towards the source valleys. The process of sediment being transported by terrestrial meltwater streams would have stopped some of the coarser sediment from entering the lake, perhaps encouraging regular varve formation at site 68. The CF III varve phase in Core 68 lasts only 25 vyr before the onset of the thinning transitional CF IV varves (at varve 217 on the master chronology).

The 'Northern' catchments (red outline in Fig. 1) represents a large area (57 + 62 km^2) as well as having multiple valley heads, so that during ice retreat, the lake received meltwater from a number of distinct valley glaciers. The position of Core 68 proximal to this complex double-catchment, with a common outflow, likely contributed to the differing varve thickness signal (including the persistence of CF IV for 96 vyr).

Our varve records show that the overdeepened, south-facing lake basins had both deglaciated at around varve 183 on the master chronology 70 vyr before the nominal onset of the Lateglacial Interstadial, and that the South Basin had deglaciated at least 254 vyr before the Lateglacial Interstadial. We also show that both lake basins were connected but had differing responses to sediment entering the lake, controlled by the bedrock high between the basins acting as a powerful sediment trap. The drop in Ca in the Itrax signal at (or tied to) vyr 209 on the master chronology indicates the point at which the glacier had retreated north of all sources of the

cessation of carbonate erosion and transport, forming the point at which the Core 64 and Core 68 local chronologies are tentatively placed on the Core 57–67 chronology. Horizontal dashed arrow indicates that the core continues, but that varve measurements are no longer reliable because the sedimentary features may be non-varve glacial outwash, or are heavily deformed. Mass transport deposits (MTD) and erosional contacts are marked, but core gaps and non-measurable varves are left blank. The tiepoints between the varve sequences of Cores 57 and 67 are shown as lettered dashed lines (the tiepoint labels T1 and T2 refer to transitions between CFs). The nominal onset of the Lateglacial Interstadial is marked at the point at which bioturbation and microfossils are seen in the sediment. A 'master' varve numbering scale has been added at the bottom for clarity of comparisons between local scales, with the caveat that the Core 64 tie is tentative and the Core 68 placement is only an 'earliest-possible' scenario. b) Itrax-derived elemental variations in calcium (pale grey dots) with a 50-point smoothed profile (dark grey, bold). The drop in Ca is shown as a black arrow in each core. (For interpretation of the references to colour in this figure legend, the reader is referred to the Web version of this article.)

Dent Group, including in the Troutbeck valley.

8.2. Deglaciation of the northern valleys of the Windermere catchment

In Cores 57 and 67, there are 36 thinning transitional varves (CF IV, Table 4; varves 206–241 on the master chronology). In Core 64 the change to CF IV has been removed by a mass transport deposit but occurs at a similar varve number. These varves are transitional between varves formed from proglacial glacier melt and varves derived from melting glacier fragments and/or snowpack, and are interpreted to have formed as ice retreated along the terrestrial valleys of the catchment. In Core 68, by contrast, the number of thinning transitional varves is 96 [+2-2], and the varve thicknesses do not match those of the other cores (Fig. 11). This indicates that ice melt events that had enough energy to deposit these transitional varves south of RM 8 only persisted for a few decades, and may also include the final stages of glacier ice disappearance in the south-facing Troutbeck Valley (Fig. 12). At least 70 vyr after the other three cores have transitioned to CF V, suggestive of a snowmelt-controlled regime, the Core 68 record still has CF IV type varves (although interspersed with CF V), which we interpret as the persistence of glacier remnants and snowpacks in at least the valley heads of the Northern Catchments.

The onset of the mm-scale snowpack/glacier remnant varves (CF V) in Cores 57, 67, and 64 occurs in vyr 242 on the master chronology. CF V persists for only 20–30 vyr in the South Basin before transitioning to CF VI (intermittent laminations), whilst in Core 64 CF V persists for 60 vyr (Fig. 11). The conditions for varve formation and preservation require strong seasonality and minimal bioturbation (Zolitschka, 2007), so the comparatively short-lived mm-scale varve sequences of the South Basin indicate rapid development of basin-wide conditions hospitable to microfauna, for example greater oxygenation, increased organic production, and reduced clastic input. In the North Basin, proximity to remnant ice sources is likely to have extended the duration of the mm-scale varve sequences. The seasonal delivery of clastic material from valley-head meltwater would have been even greater at Core 68 than Core 64, with CF V persisting in Core 68 at least 111 vyr after Core 64 and 158 vyr into the early Lateglacial Interstadial. The earlier cessation of CF V varve formation in the south therefore likely reflects increasing distance from the primary sediment source. Site 68 is also most prone to lamina preservation in the modern lake due to a tendency to dysoxia (Fielding et al., 2018) on account of deeper water (54 m).

The seismic reflection section for the location of Core 68 shows that the corer penetrated down to ~2.5 m above the SF I unit (interpreted as over-consolidated till; Fig. 2), such that the disturbed basal sediments at the bottom of the core were likely deposited not long after the ice retreated past the core location. The varve chronology in Core 68 spans 221 vyr, in addition to the proximal glacial outwash of CF I and the chaotic, poorly laminated sediment of CF II (Table 4). The time between exposure of the Core 68 site and the cessation of varves is likely to have been less than ~250 years.

8.3. Glacier retreat rates

Water-terminating glaciers, particularly in overdeepened basins, usually retreat faster than land-terminating glaciers, since they often have calving margins, and lose mass from both surface and subaqueous (sometimes temperature-driven) melt with less friction from grounding (Carr et al., 2017; Chernos et al., 2016). The glacier retreat along the overdeepened Windermere valley (between the RMs) was therefore likely faster than the subsequent retreat into the upland source valleys, so we estimate these phases separately.

In the South Basin, neither core reached the bottom varve so the retreat rate along the South Basin is not possible to estimate, although approximate ice margin locations through time given by the thickness of different seismic facies (SF) are indicated in Fig. 12. For retreat along the North Basin, we can use the Core 64 varve chronology. The thick, coarse-based CF II varves of Core 64 indicate a very proximal ice margin, but we do not know the degree of this proximity: RM 8, RM 9, or somewhere in between? We also do not know exactly where the ice margin lay when the transitions between CFs occurred, although the suggestion that the transition to CF III varves in the North Basin (vyr 183) represents the glacier becoming terrestrial is reasonable. The drop in Ca (vyr 209) indicates the point at which the glacier had retreated north of all sources of the Dent Group; that this point lay ~2.5 km beyond the northern margin of the lake. We can therefore estimate a range of retreat rates along the North Basin using RM 8 and RM 9 as the minimum and maximum southern ice margin bounds, and using varve 183 as the northern ice margin bound, the northern shore of the modern lake. The Core 64 chronology has 50 vyr before vyr 183, although there is some uncertainty about the number of varves in core gaps. The distance from RM 8 to the northern lake shore is ~5700 m, and the distance from RM 9 is 3500 m. This gives an approximate rate range of 70–114 m yr^{-1}. The coarseness and thickness of the bottom varves of Core 64 strongly suggests that the ice margin was much closer to RM 8 than 9, although it was probably already in retreat-so the rate is likely closer to, but below, the upper value (around 110 m yr^{-1}?). This estimate neither supports nor rules out the DGMs being annual: if annual, the DGMs would represent ice retreat of ~120 m yr^{-1}. However, we do not know the length of any stillstand at RM 9, so the calculated rate of 114 m yr^{-1} from RM 8 could represent a gradual retreat and short stillstand, or could represent stepped annual retreat at 120 m yr^{-1} with a stillstand of 3 years at RM 9 (Fig. 12). If the ice margin were already some way north of RM 8 by varve 133, which is likely, the stillstand at RM 9 would just be longer.

The retreat rate into the catchment valleys can be split by the drop in Ca (vyr 209). Vyr 183–209 is 27 vyr, and the distance from the northern lake shore to the point beyond any Dent Group outcrops (including in Pull Wyke, a nearby small but limestone-rich tributary valley; Figs. 1 and 12) is ~2.5 km. This gives an initial terrestrial retreat rate of 92.5 m yr^{-1}. For the next segment of retreat, the simplest calculation uses the length of the Core 68 varve chronology after the Ca marker (203 vyr) and the distance to the watershed, which is ~10 km. This gives an average rate of 49.3 m yr^{-1}. This calculation assumes that the last varve in Core 68 coincides with the last disappearance of valley-head ice. We know that the restricted catchment ice extent of the Younger Dryas also gave rise to mm-scale varves in Windermere (Avery, 2017; Pennington, 1947, 1943). However, varves have been shown to be produced in modern high-latitude unglaciated catchments (Francus et al., 2008; Hambley and Lamoureux, 2006; Kaufman et al., 2011), so ice may have disappeared before the final CF V varve, giving a faster rate.

The estimated average lake-terminating rate of retreat in Windermere (110–120 m yr^{-1}) is 2.3 x that of the land-terminating phase (49 m yr^{-1} or a little faster), which is reasonable, since a study of 54 modern-day outlet glaciers on Nova Zemlya found that water-terminating glaciers retreated on average ~3.5 x faster than land-terminating glaciers (Carr et al., 2017). The fast water-terminating retreat rate (70–114 m yr^{-1}, or 120 m yr^{-1} + stillstand) may be due to the south-facing, overdeepened 'ribbon' nature of the basins and the late stage of retreat relative to the LGM. Bridge Glacier, a modern-day calving outlet glacier in

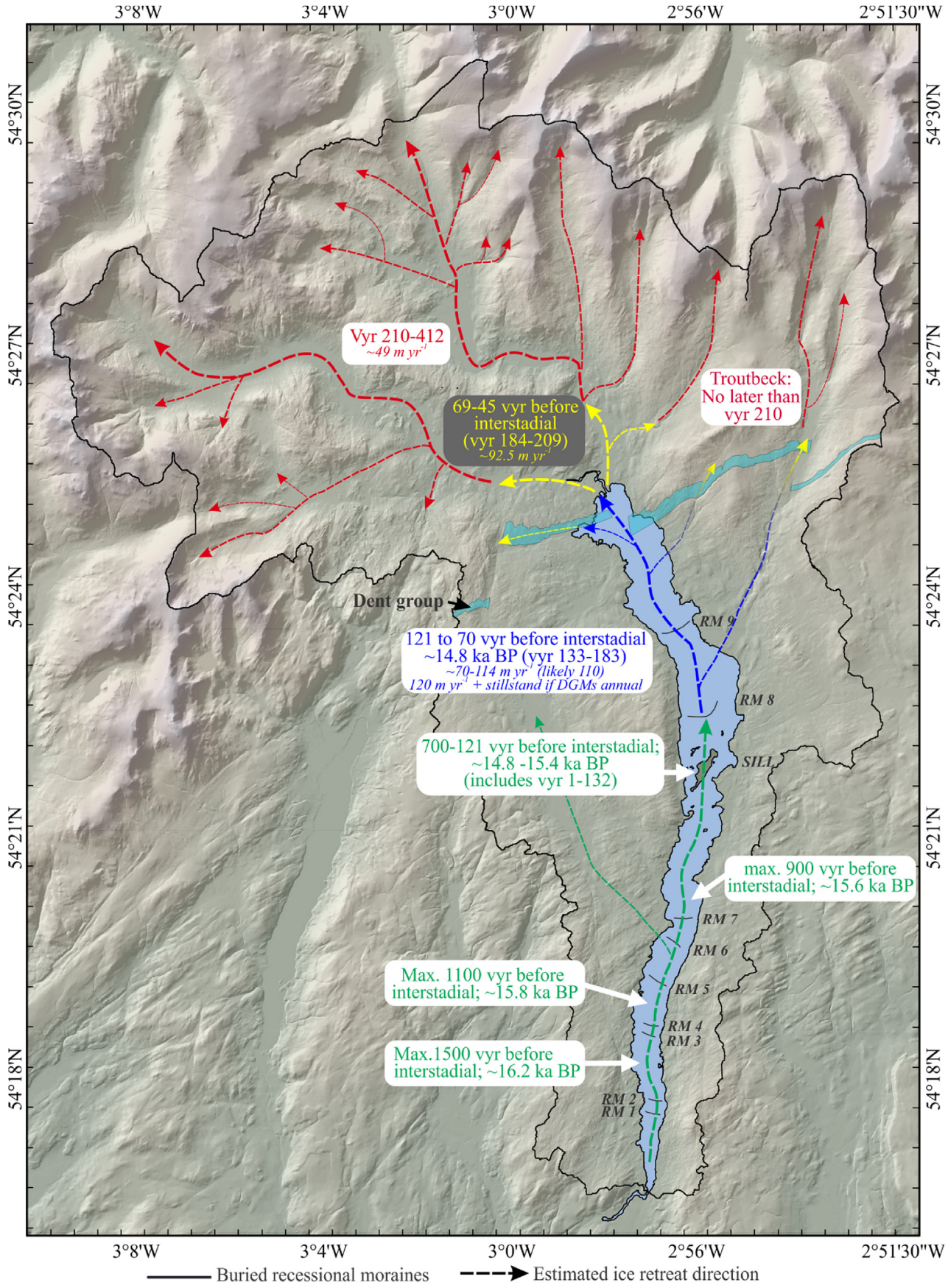

Fig. 12. A demonstrative schematic of ice retreat in the Windermere catchment, with lake basin retreat timings based on seismic evidence (see section 8.4) and varve chronologies, and terrestrial valley retreat based on a varve chronology. Topography derived from 1- and 2 m LiDAR datasets and NEXTMap data. Buried recessional moraines (RMs) are shown as solid black lines and labelled, and estimated ice retreat directions are shown as dashed arrows. The Dent Group (formerly Coniston Limestone) is shown in turquoise. Contains UK Environment Agency data © Environment Agency copyright and/or database right 2015. All rights reserved.

British Columbia with a similar length to that of Windermere's (but with a smaller area of 64 km^2), since 1991 has exhibited retreat rates of 144 m yr^{-1} and up to 400 m yr^{-1} (Chernos et al., 2016), so a water-terminating retreat rate (from just prior to the rapid warming) of 120 m yr^{-1} for Windermere is reasonable.

The Windermere land-terminating retreat rate is considerably faster than the few existing estimates of terrestrial glacier retreat from elsewhere in the BIIS. Estimates for post-LGM valley glacier retreat rates from southern Wales at Glacial Lake Llangorse are 5.2 m yr^{-1} (Palmer et al., 2008) although this likely occurred much earlier than at Windermere. Retreat rate estimates from southern Donegal, north-western Ireland, between ~17–15 ka BP are somewhat higher at 12–24 m yr^{-1}, but these are from a much larger body of ice than an outlet glacier so do not provide a direct comparison (Wilson et al., 2019). The average terrestrial retreat rate is comparable to present-day retreating Alpine valley glaciers (usually up to ~50 m yr^{-1}), including the Grosser Aletsch glacier in the Swiss Alps that has a catchment size of 116 km^2 (compared with 119 km^2 for Windermere's 'northern valleys') where some individual years have seen retreats of >100 m (Glaciological reports, 2017; Swiss Glacier Monitoring Network, 2017). The estimated Windermere terrestrial retreat rates are a response to the period of rapid warming at the commencement of the Lateglacial Interstadial and the similarity to the modern day retreat rates, highlight the rapidity of this warming.

8.4. Broader significance and potential of the Windermere record

The four new Windermere cores, together with the extensive seismic stratigraphic data, demonstrate that there is a contiguous and coherent high-resolution sedimentary record of environmental change in the North of England through the last deglaciation. It is clear that the full extent of the lake record has been only partly realised with the present core suite. Below Core 67 there is another ~13 m of SF II (seismic facies interpreted as glaciolacustrine sedimentation; Pinson et al., 2013), and 2.25 km farther south in the depocentre containing Core 57, there exists another ~16 m of SF II below the depth of core penetration (Fig. 2). Extrapolating through the remaining SF II varved facies, using the average thickness of the bottom 20 varves in Cores 57 and 67, suggests the presence of up to ~650 further varves below Core 67, and up to ~800 further varves in the depocentre of Core 57. These values represent a maximum, since varves are very likely to become thicker in the deeper sediment; the deepest sediment would probably represent thickly-bedded CF II and non-varved CF I.

A depocentre some 1.45 km south of Core 57 between RMs 2 and 3 contains a total of 12 m of SF IIb and 34 m of SF IIa (Fig. 13), representing a further 46 m of sediment in total. The excellent match between the varve records of Cores 67 and 57, from sub-basins 2.25 km apart, provides confidence in potential varve correlations with the other sub-basins of Windermere's South Basin. Extrapolating through the remaining 9 m of SF IIb varved facies in the southern depocentre, again using the average thickness of the bottom 20 varves in Cores 57 and 67, suggests the presence of ~450 further varves within the SF IIb section alone. Below this, there is a further 34 m of SF IIa, which is known in the North Basin to also include varves (Cores 64 and 68), suggesting there may be potential for a considerably longer total varve chronology in the South Basin extending further back into Heinrich Stadial 1 (GS-2).

SF IIb in the South Basin represents sedimentation when the

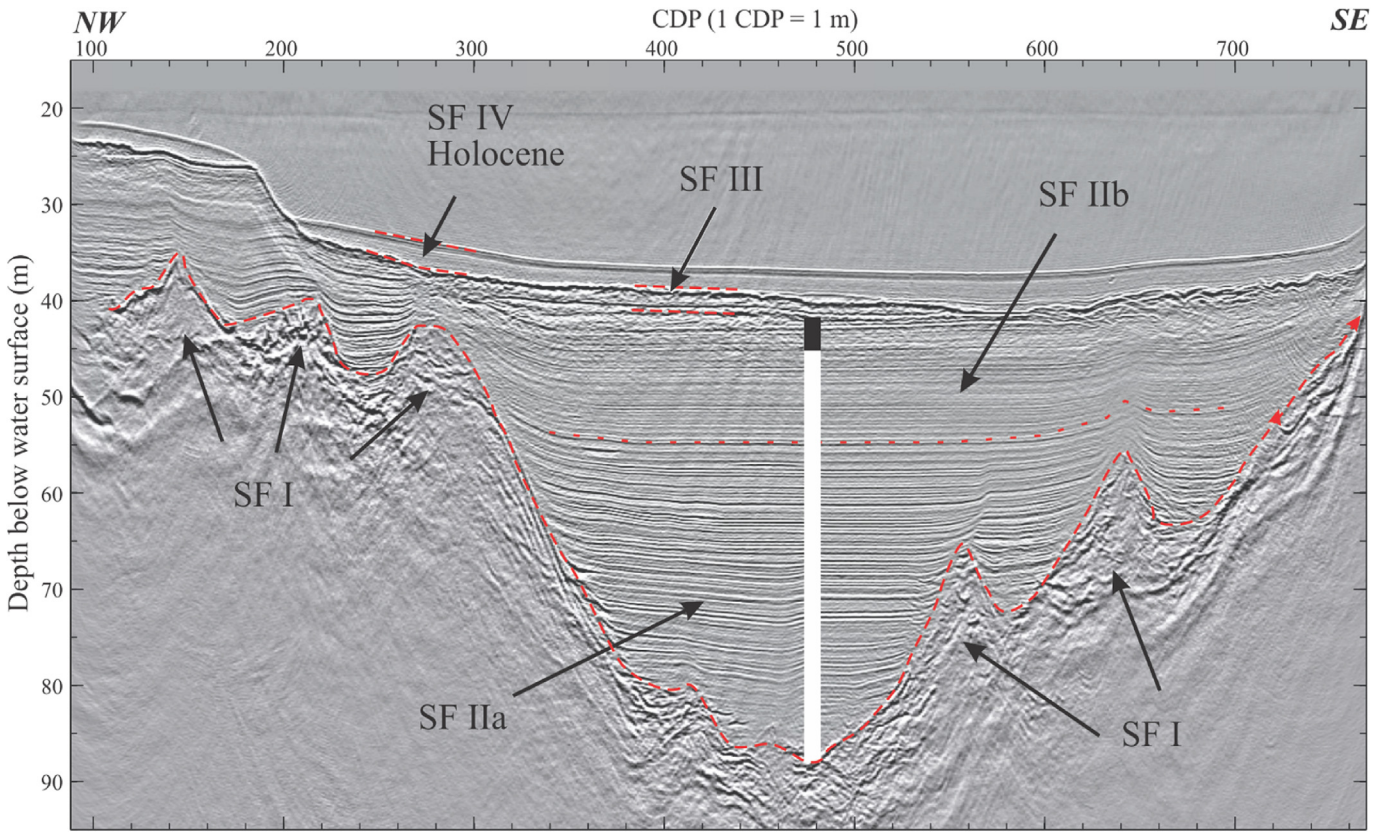

Fig. 13. The potential extent of a Windermere varve suite through the Heinrich Stadial 1. Interpreted depth-migrated seismic reflection section through a promising depocentre between Recessional Moraines 2 and 3 in the South Basin (Fig. 2a). Vertical bar indicates example extent of core penetrations in this study, where the white section represents potential varves beyond the scope of the 2012 coring campaign. Seismic facies (SF) are indicated with arrows and separated by dashed lines; a dotted line separates SF IIa and IIb.

glacier terminus was already north of the sill between the two basins, trapping coarser material. Seismic and core evidence indicates that the glacier terminus had retreated north of this sill at least 255 vyr, and a maximum of 700 vyr, before sedimentary evidence for climate amelioration in the Windermere catchment (e.g. macro- and microfossils; bioturbation of varves; Fig. 11). The sill may have facilitated a prolonged stillstand at this point by grounding the glacier. Adding the 34 m of SF IIa seen in the seismic reflection section in the South Basin (Fig. 13) shows that the depocentre (approximately a third of the way north along the South Basin) started deglaciating potentially 1000–1500 vyr (SF IIa) prior to the onset of the Lateglacial Interstadial. Drilling in the different sub-basins between the moraine ridges in the South Basin could provide several more long cores from this period with an annually-resolved internal chronology, which as well as constraining the glacial retreat timings for RMs 1 through 7, could also be a trove of palaeoclimate information for Heinrich Stadial 1.

Exposure dating from some other Lake District valleys indicate that some valley glaciers survived until ~15 ka BP (Wilson et al., 2018), suggesting that the other larger valley glaciers of the Lake District may have deglaciated on a similar timescale to that of Windermere. This suggestion is in accordance with the Donegal Ice Centre in north-west Ireland, and the Galloway Ice Centre in south-west Scotland, where in both cases the ice centres shrunk and had mostly deglaciated by 15 ka BP but (at least in Ireland) glacial remnants in valley heads persisted into the early Lateglacial Interstadial (Ballantyne et al., 2013; Wilson et al., 2019). Tomkins et al. (2018) presents similar results from the Wicklow Mountains in eastern Ireland, and collectively with evidence from other locations proposes that many upland ice centres surrounding the Irish Sea Basin downwasted rapidly after the LGM, transitioning to alpine-style glaciation, but that valley glaciers or cirques may have persisted until the onset of the Lateglacial Interstadial. This also agrees with evidence from southern Wales (Glasser et al., 2018) and earlier models suggesting widespread deglaciation prior to the Lateglacial Interstadial warming (Clark et al., 2012). The results from Windermere also support this model, with the LDIC shrinking rapidly after separation from the BIIS (16.4–15.7 ka BP), transitioning to alpine-style glaciation (South Basin terminus); then a rapid valley glacier retreat (North Basin terminus) starting 255–700 yr prior to the Lateglacial Interstadial hemispheric warming event (14.7 ka BP), leaving only persistent glacial remnants in the upper valleys during the early interstadial. Ribbon lakes from these upland ice caps, overdeepened by topography-driven glacial erosion, also have the potential to provide similar high-resolution palaeoclimate archives.

9. Conclusions

In this study, a seismic stratigraphic survey resolving four distinct glacial – post-glacial sediment units is integrated with a suite of cored sediment records from Windermere, in order to constrain the retreat behaviour of the Lake District ice cap and examine the potential of Windermere as a long, annual-resolution palaeo-climate archive. Long sequences of laminated sediments in cores from along the lake basins have been identified as varves. Previous work in this area identified a sequence of buried recessional and De Geer moraines in the Windermere lakebed which were interpreted as a stepped retreat of ice northwards along the Windermere valley, but no ages are available for the moraines (Pinson et al., 2013). Our work has shown that:

- A new >400 varve year (vyr) varve chronology of two floating parts documents ice retreat along the source valleys of the Windermere catchment.
- A combination of seismic and grain size evidence suggests that the valley glacier had retreated north of the bedrock high currently separating the lake into two basins between 255 and (max.) 700 vyr prior to the Lateglacial Interstadial, and a 46 m sediment depocentre in the south Basin suggests that the lake valley may have started deglaciating up to a maximum of 1500 years prior to the Lateglacial Interstadial (~16.2 ka BP).
- The glacier had retreated to the northern end of the lake basins by at least 70 vyr prior to the Interstadial. The sill between the basins acted as a powerful sediment trap, leading to the South Basin exhibiting a uniform response to glacial melt.
- Ice retreat rates for the glacier in its lake-terminating and land-terminating phases were estimated using the varve chronologies. The terrestrial rate was 49 m yr^{-1}, perhaps faster. The preceding lake-terminating phase gave a range of 70–114 m yr^{-1} (most likely at the upper end), although this could also be interpreted as 120 m yr^{-1} between potentially annual De Geer moraines and a stillstand of $\geq$3 vyr at Recessional Moraine 9.
- The northernmost varve record extends for at least 111 vyr beyond (i.e. subsequent to) the main chronology. We infer that the proximity of this core to persistent glacier remnants and snowpacks promoted varve formation at this location at least 158 vyr into the early Lateglacial Interstadial.
- Further coring of Windermere, between each RM and down to the first varve in each sequence, would enable study of ice retreat rates along the entire lake, and, given the thicknesses of some of the South Basin depocentres, produce an annually-resolved palaeoclimate archive that extends further into Heinrich Stadial 1.
- We have demonstrated the potential of UK overdeepened ribbon lakes to yield pre-Interstadial varve chronologies with respect to the deglaciation of the British Isles, and we anticipate and encourage further coring campaigns both in Windermere and in UK lakes and lochs in future.

Acknowledgements

We are grateful to Richard and Daniel Niederreiter, Helen Miller, John Davis, and Stuart Jarvis for their support during sediment coring, and to the BGS marine operations crew and hydrographic surveyors of the R/V White Ribbon. We thank Martin Dodgson and the Windermere Lake Wardens for their assistance, as well as the Freshwater Biological Association.

Charlotte Bryant advised on radiocarbon dating. This work was supported by the NERC Radiocarbon Facility NRCF010001 (allocation numbers 1746.1013 and 1856.1014), the BGS University Funding Initiative (Reference S243), and the University of Southampton.

We are grateful to Pete Langdon and Sarah Greenwood who provided constructive comments on the manuscript informally, and to Neil Roberts and two anonymous reviewers who provided much-appreciated constructive criticism in the peer review process.

We are grateful to Matt Cooper, Suzanne Maclachlan, Charlie Thompson, and Ross Williams for their technical expertise and lab assistance.

Carol J Cotterill publishes with the permission of the Executive Director of the British Geological Survey, Natural Environment Research Council.

Appendix A. Supplementary data

Supplementary data to this article can be found online at https://doi.org/10.1016/j.quascirev.2019.105894.

References

Agassiz, L., 1840. On glaciers, and the evidence of their having once existed in Scotland, Ireland, and England. Proc. Geol. Soc. Lond. 3, 327–332.

Amann, B., Mauchle, F., Grosjean, M., 2014. Quantitative high-resolution warm season rainfall recorded in varved sediments of Lake Oeschinen, northern Swiss Alps: calibration and validation AD 1901-2008. J. Paleolimnol. 51, 375–391. https://doi.org/10.1007/s10933-013-9761-3.

Avery, R.S., 2017. High-Resolution Records of Deglaciation and Palaeomagnetism in the Late- Quaternary Sediments of Windermere. Thesis. University of Southampton, UK.

Avery, R.S., Kemp, A.E.S., Bull, J.M., Pearce, R.B., Vardy, M.E., Fielding, J.J., Cotterill, C.J., 2019. Dataset for "A new varve sequence from Windermere, UK, records rapid ice retreat prior to the Lateglacial Interstadial (GI-1)". https://doi.org/10.5258/SOTON/D1054. https://eprints.soton.ac.uk/433426/.

Avery, R.S., Xuan, C., Kemp, A.E.S., Bull, J.M., Cotterill, C.J., Fielding, J.J., Pearce, R.B., Croudace, I.W., 2017. A new Holocene record of geomagnetic secular variation from Windermere, UK. Earth Planet. Sci. Lett. 477, 108–122. https://doi.org/10.1016/j.epsl.2017.08.025.

Ballantyne, C.K., Rinterknecht, V., Gheorghiu, D.M., 2013. Deglaciation chronology of the Galloway Hills ice centre, southwest Scotland. J. Quat. Sci. 28, 412–420. https://doi.org/10.1002/jqs.2635.

Ballantyne, C.K., Stone, J.O., Fifield, L.K., 2009. Glaciation and deglaciation of the SW Lake District, England: implications of cosmogenic 36Cl exposure dating. Proc. Geol. Assoc. 120, 139–144. https://doi.org/10.1016/j.pgeola.2009.08.003.

Bendle, J.M., Palmer, A.P., Thorndycraft, V.R., Matthews, I.P., 2017. High-resolution chronology for deglaciation of the patagonian ice sheet at Lago Buenos Aires (46.5°S) revealed through varve chronology and Bayesian age modelling. Quat. Sci. Rev. 177, 314–339. https://doi.org/10.1016/j.quascirev.2017.10.013.

Björck, S., Wohlfarth, B., 2001. 14C chronostratigraphic techniques in paleolimnology. In: Last, W.M., Smol, J.P. (Eds.), Tracking Environmental Change Using Lake Sediments. Kluwer Academic Publishers, Dordrecht, pp. 557–578. https://doi.org/10.1007/978-94-007-2745-8.

Blass, A., Anselmetti, F., Ariztegui, D., 2003. 60 years of glaciolacustrine sedimentation in Steinsee (Sustenpass, Switzerland) compared with historic events and instrumental meteorological data. In: Lake Systems from the Ice Age to Industrial Time. Eclogae Geologicae Helvetiae/Swiss Journal of Geosciences, Birkhäuser, Basel, pp. 59–71. https://doi.org/10.1007/978-3-0348-7992-7_8.

Blott, S.J., Pye, K., 2001. Gradistat: a grain size distribution and statistics package for the analysis of unconsolidated sediments. Earth Surf. Process. Landforms 26, 1237–1248.

Blystad, P., Selsing, L., 1989. Some erroneous radiocarbon dates of lacustrine sediments. Nor. Geol. Tidsskrif 69, 201–208.

Bouvier, V., Johnson, M.D., Påsse, T., 2015. Distribution, genesis and annual-origin of De Geer moraines in Sweden: insights revealed by LiDAR. GFF 137, 319–333. https://doi.org/10.1080/11035897.2015.1089933.

Brothers, R.J., Kemp, A.E.S., Maltman, A.J., 1996. Mechanical development of vein structures due to the passage of earthquake waves through poorly-consolidated sediments. Tectonophysics 260, 227–244. https://doi.org/10.1016/0040-1951(96)00088-1.

Brown, V.H., 2009. Reconstructing Loch Lomond Stadial Glaciers and Climate in the South-West English Lake District. Thesis. University of Durham.

Buckland, W., 1840. A memoir on the evidences of glaciers in Scotland and the north of England. Proc. Geol. Soc. Lond. 3 (332–337), 345–348.

Carr, J.R., Bell, H., Killick, R., Holt, T., 2017. Exceptional retreat of Novaya Zemlya ' s marine-terminating outlet glaciers between 2000 and 2013. Cryosphere 11, 2149–2174. https://doi.org/10.5194/tc-11-2149-2017.

Chernos, M., Koppes, M., Moore, R.D., 2016. Ablation from calving and surface melt at lake-terminating Bridge Glacier, British Columbia, 1984-2013. Cryosphere 10, 87–102. https://doi.org/10.5194/tc-10-87-2016.

Chiverrell, R.C., Burke, M.J., Thomas, G.S.P., 2016. Morphological and sedimentary responses to ice mass interaction during the last deglaciation. J. Quat. Sci. 31, 265–280. https://doi.org/10.1002/jqs.2864.

Chiverrell, R.C., Smedley, R.K., Small, D., Ballantyne, C.K., Burke, M.J., Callard, S.L., Clark, C.D., Duller, G.A.T., Evans, D.J.A., Fabel, D., van Landeghem, K., Livingstone, S.J., Ó Cofaigh, C., Thomas, G.S.P., Roberts, D.H., Saher, M., Scourse, J.D., Wilson, P., 2018. Ice margin oscillations during deglaciation of the northern Irish Sea Basin. J. Quat. Sci. 33, 739–762. https://doi.org/10.1002/jqs.3057.

Chutko, K.J., Lamoureux, S.F., 2008. Identification of coherent links between interannual sedimentary structures and daily meteorological observations in Arctic proglacial lacustrine varves: potentials and limitations. Can. J. Earth Sci. 45, 1–13. https://doi.org/10.1139/E07-070.

Clark, C.D., Hughes, A.L.C., Greenwood, S.L., Jordan, C., Sejrup, H.P., 2012. Pattern and timing of retreat of the last British-Irish Ice Sheet. Quat. Sci. Rev. 44, 112–146. https://doi.org/10.1016/j.quascirev.2010.07.019.

Clark, P.U., Dyke, A.S., Shakun, J.D., Carlson, A.E., Clark, J., Wohlfarth, B., Mitrovica, J.X., Hostetler, S.W., McCabe, A.M., 2009. The last glacial maximum. Science 325, 710–714. https://doi.org/10.1126/science.1172873.

Cockburn, J.M.H., Lamoureux, S.F., 2007. Century-scale variability in late-summer rainfall events recorded over seven centuries in subannually laminated lacustrine sediments, White Pass, British Columbia. Quat. Res. 67, 193–203. https://doi.org/10.1016/j.yqres.2006.10.003.

Coope, G.R., Pennington, W., 1977. The Windermere interstadial of the late Devensian. Philos. Trans. R. Soc. Lond. B 280, 337–339.

De Geer, G., 1937. A New Varve connection between four continents. Ark. Mat. Astron. Och Fys. 25 B.

De Geer, G., 1912. A geochronology of the last 12000 years. Proc. Int. Geol. Congr. Stock. 1, 241–257.

Devine, R.M., Palmer, A.P., 2017. A new varve thickness record from Allt Bhraic Achaidh Fan, middle Glen Roy, Lochaber: implications for understanding the Loch Lomond Stadial glaciolacustrine varve sedimentation trends. Proc. Geol. Assoc. 128, 136–145. https://doi.org/10.1016/j.pgeola.2016.07.008.

Fielding, J.J., Kemp, A.E.S., Bull, J.M., Cotterill, C.J., Pearce, R.B., Avery, R.S., Langdon, P.G., Croudace, I.W., 2018. Palaeoseismology from microfabric and geochemical analysis of lacustrine sediments, Windermere, UK. J. Geol. Soc. Lond. 175, 903–914. https://doi.org/10.1144/jgs2017-094.

Francus, P., Bradley, R.S., Lewis, T., Abbott, M.B., Retelle, M., Stoner, J.S., 2008. Limnological and sedimentary processes at Sawtooth Lake, Canadian High Arctic, and their influence on varve formation. J. Paleolimnol. 40, 963–985. https://doi.org/10.1007/s10933-008-9210-x.

Francus, P., Keimig, F., Besonen, M., 2002. An algorithm to aid varve counting and measurement from thin-sections. J. Paleolimnol. 28, 283–286. https://doi.org/10.1023/A:1021624415920.

Friedman, G.M., Sanders, J.E., 1978. Principles of Sedimentology, first ed. Wiley.

Gammon, P.R., Neville, L.A., Patterson, R.T., Savard, M.M., Swindles, G.T., 2017. A log-normal spectral analysis of inorganic grain-size distributions from a Canadian boreal lake core: towards refining depositional process proxy data from high latitude lakes. Sedimentology 64, 609–630. https://doi.org/10.1111/sed.12281.

Glaciological reports, 2017. The Swiss Glaciers 2013/14 and 2014/15. Zurich. http://doi.org/10.18752/glrep 135-136.

Glasser, N.F., Davies, J.R., Hambrey, M.J., Davies, B.J., Gheorghiu, D.M., Balfour, J., Smedley, R.K., Duller, G.A.T., 2018. Late Devensian deglaciation of south-west Wales from luminescence and cosmogenic isotope dating. J. Quat. Sci. 33, 804–818. https://doi.org/10.1002/jqs.3061.

Hambley, G.W., Lamoureux, S.F., 2006. Recent summer climate recorded in complex varved sediments, Nicolay Lake, Cornwall Island, Nunavut, Canada. J. Paleolimnol. 35, 629–640. https://doi.org/10.1007/s10933-005-4302-3.

Holmquist, B., Wohlfarth, B., 1998. An evaluation of the late weichselian Swedish varve chronology based on cross-correlation analysis. GFF 120, 35–46. https://doi.org/10.1080/11035899801201035.

Hughen, K.A., Overpeck, J.T., Anderson, R.F., Williams, K.M., 1996. The potential for palaeoclimate records from varved Arctic lake sediments: Baffin Island, Eastern Canadian Arctic. Geol. Soc. Lond. Spec. Publ. 116, 57–71. https://doi.org/10.1144/GSL.SP.1996.116.01.07.

Hughes, A.L.C., Clark, C.D., Jordan, C.J., 2014. Flow-pattern evolution of the last British ice sheet. Quat. Sci. Rev. 89, 148–168. https://doi.org/10.1016/j.quascirev.2014.02.002.

Hughes, A.L.C., Gyllencreutz, R., Lohne, Ø.S., Mangerud, J., Svendsen, J.I., 2016a. The last Eurasian ice sheets - a chronological database and time-slice reconstruction, DATED-1. Boreas 45, 1–45. https://doi.org/10.1111/bor.12142.

Hughes, P.D., Glasser, N.F., Fink, D., 2016b. Rapid thinning of the Welsh Ice Cap at 20-19 ka based on 10Be ages. Quat. Res. 85, 107–117. https://doi.org/10.1016/j.yqres.2015.11.003.

Hutchinson, I., James, T.S., Reimer, P.J., Bornhold, B.D., Clague, J.J., 2004. Marine and limnic radiocarbon reservoir corrections for studies of late- and postglacial environments in Georgia Basin and Puget Lowland, British Columbia, Canada and Washington, USA. Quat. Res. 61, 193–203. https://doi.org/10.1016/j.yqres.2003.10.004.

Kaufman, C.a., Lamoureux, S.F., Kaufman, D.S., 2011. Long-term river discharge and multidecadal climate variability inferred from varved sediments, southwest Alaska. Quat. Res. 76, 1–9. https://doi.org/10.1016/j.yqres.2011.04.005.

Knight, J., 2001. Glaciomarine deposition around the Irish Sea basin: some problems and solutions. J. Quat. Sci. 16, 405–418. https://doi.org/10.1002/jqs.630.

Lamoureux, S.F., 2001. Varve chronology techniques. In: Last, W.M., Smol, J.P. (Eds.), Tracking Environmental Change Using Lake Sediments. Volume 1: Basin Analysis, Coring, and Chronological Techniques. Kluwer Academic Publishers, Dordrecht, pp. 247–260.

Livingstone, S.J., Evans, D.J.A., Ó Cofaigh, C., 2010a. Re-advance of Scottish ice into the Solway lowlands (Cumbria, UK) during the main late Devensian deglaciation. Quat. Sci. Rev. 29, 2544–2570. https://doi.org/10.1016/j.quascirev.2010.04.007.

Livingstone, S.J., Ócofaigh, C., Evans, D.J.A., Palmer, A.P., 2010b. Sedimentary evidence for a major glacial oscillation and proglacial lake formation in the Solway Lowlands (Cumbria, UK) during Late Devensian deglaciation. Boreas 39, 505–527. https://doi.org/10.1111/j.1502-3885.2010.00149.x.

Livingstone, S.J., Roberts, D.H., Davies, B.J., Evans, D.J.A., Ó Cofaigh, C., Gheorghiu, D.M., 2015. Late Devensian deglaciation of the Tyne gap palaeo-ice stream, northern England. J. Quat. Sci. 30, 790–804. https://doi.org/10.1002/jqs.2813.

Lord, T.C., O'Connor, T.P., Siebrant, D.C., Jacobi, R.M., 2007. People and large carnivores as biostratinomic agents in Lateglacial cave assemblages. J. Quat. Sci. 22, 681–694. https://doi.org/10.1002/jqs.1101.

Lowag, J., Bull, J.M., Vardy, M.E., Miller, H., Pinson, L.J.W., 2012. High-resolution seismic imaging of a Younger Dryas and Holocene mass movement complex in glacial lake Windermere, UK. Geomorphology 171–172, 42–57. https://doi.org/10.1016/j.geomorph.2012.05.002.

Lowe, J., Walker, M., 2000. Radiocarbon dating the last glacial interglacial transition (ca. 14–9 14C ka BP) in terrestrial and marine records: the need for new quality

assurance protocols. Radiocarbon 42, 53–68.
McDougall, D.a., 2001. The geomorphological impact of loch lomond (younger Dryas) Stadial plateau icefields in the central Lake District, northwest England. J. Quat. Sci. 16, 531–543. https://doi.org/10.1002/jqs.624.
McGowan, S., Barker, P., Haworth, E.Y., Leavitt, P.R., Maberly, S.C., Pates, J., 2012. Humans and climate as drivers of algal community change in Windermere since 1850. Freshw. Biol. 57, 260–277. https://doi.org/10.1111/j.1365-2427.2011.02689.x.
McNamara, K.J., 1979. The age, stratigraphy and genesis of the Coniston limestone group in the southern Lake District. Geol. J. 14, 41–68. https://doi.org/10.1002/gj.3350140104.
Menounos, B., Clague, J.J., 2008. Reconstructing hydro-climatic events and glacier fluctuations over the past millennium from annually laminated sediments of Cheakamus Lake, southern Coast Mountains, British Columbia, Canada. Quat. Sci. Rev. 27, 701–713. https://doi.org/10.1016/j.quascirev.2008.01.007.
Miller, H., 2014. Lake Bed Environments, Modern Sedimentation and the Glacial and Post-glacial History of Windermere. University of Southampton, UK.
Miller, H., Bull, J.M., Cotterill, C.J., Dix, J.K., Winfield, I.J., Kemp, A.E.S., Pearce, R.B., 2013. Lake bed geomorphology and sedimentary processes in glacial lake Windermere, UK. J. Maps 9, 299–312. https://doi.org/10.1080/17445647.2013.780986.
Miller, H., Cotterill, C.J., Bradwell, T., 2014a. Glacial and paraglacial history of the Troutbeck Valley, Cumbria, UK: integrating airborne LiDAR, multibeam bathymetry, and geological field mapping. Proc. Geol. Assoc. 125, 31–40. https://doi.org/10.1016/j.pgeola.2013.04.007.
Miller, H., Winfield, I.J., Fletcher, J.M., Ben James, J., van Rijn, J., Bull, J.M., Cotterill, C.J., 2014b. Distribution, characteristics and condition of Arctic charr (Salvelinus alpinus) spawning grounds in a differentially eutrophicated twin-basin lake. Ecol. Freshw. Fish 24, 32–43. https://doi.org/10.1111/eff.12122.
Moore, J.J., Hughen, K.A., Miller, G.H., Overpeck, J.T., 2001. Little ice age recorded in summer temperature reconstruction from vared sediments of donard lake, Baffin island, Canada. J. Paleolimnol. 25, 503–517. https://doi.org/10.1023/A:1011181301514.
Mosely, F., 1984. Lower palaeozoic lithostratigraphical classification in the English Lake District. Geol. J. 19, 239–247.
Nolan, S.R., Bloemendal, J., Boyle, J., Jones, R., Oldfield, F., 1999. Mineral magnetic and geochemical records of late Glacial climatic change from two northwest European carbonate lakes S. J. Paleolimnol. 22, 97–107. https://doi.org/10.1023/A.
O'Connor, T., Lord, T., 2013. Cave palaeontology. In: Caves and Karst of the Yorkshire Dales. British Cave Research Association, Buxton, pp. 225–238.
Ó Cofaigh, C., Weilbach, K., Lloyd, J.M., Benetti, S., Callard, S.L., Chiverrell, R.C., Dunlop, P., Saher, M., Livingstone, S.J., Katrien, J.J., 2019. Early deglaciation of the British-Irish Ice Sheet on the Atlantic shelf northwest of Ireland driven by glacioisostatic depression and high relative sea level. Quat. Sci. Rev. 208, 1–50. https://doi.org/10.1016/j.quascirev.2018.12.022.
Ojala, A.E.K., Francus, P., Zolitschka, B., Besonen, M., Lamoureux, S.F., 2012. Characteristics of sedimentary varve chronologies – a review. Quat. Sci. Rev. 43, 45–60. https://doi.org/10.1016/j.quascirev.2012.04.006.
Oldfield, F., 2013. Mud and magnetism: records of late Pleistocene and Holocene environmental change recorded by magnetic measurements. J. Paleolimnol. 49, 465–480. https://doi.org/10.1007/s10933-012-9648-8.
Palmer, A.P., Rose, J., Lowe, J.J., MacLeod, A.M., 2010. Annually resolved events of younger Dryas glaciation in Lochaber (glen roy and glen spean), western Scottish Highlands. J. Quat. Sci. 25, 581–596. https://doi.org/10.1002/jqs.1370.
Palmer, A.P., Rose, J., Lowe, J.J., Walker, M.J.C., 2008. Annually laminated late pleistocene sediments from Llangorse lake, south Wales, UK: a chronology for the pattern of ice wastage. Proc. Geol. Assoc. 119, 245–258. https://doi.org/10.1016/S0016-7878(08)80304-5.
Palmer, A.P., Rose, J., Rasmussen, S.O., 2012. Evidence for phase-locked changes in climate between Scotland and Greenland during GS-1 (Younger Dryas) using micromorphology of glaciolacustrine varves from Glen Roy. Quat. Sci. Rev. 36, 114–123. https://doi.org/10.1016/j.quascirev.2011.12.003.
Patton, H., Hubbard, A., Andreassen, K., Auriac, A., Whitehouse, P.L., Stroeven, A.P., Shackleton, C., Winsborrow, M., Heyman, J., Hall, A.M., 2017. Deglaciation of the Eurasian ice sheet complex. Quat. Sci. Rev. 169, 148–172. https://doi.org/10.1016/j.quascirev.2017.05.019.
Pennington, W., 1977. The late Devensian flora and vegetation of Britain. Philos. Trans. R. Soc. Lond. B 280, 247–271. Frequency based selection occurs when the relative fitness of an allele changes dependent on its frequency, and the frequency of other alleles, within the population.
Pennington, W., 1973. Glaciation-the shaping of the landscape. In: The Lake District: A Landscape History. Collins, London.
Pennington, W., 1947. Studies of the post-glacial history of British vegetation. VII. Lake sediments: pollen diagrams from the bottom deposits of The north Basin of Windermere. Philos. Trans. R. Soc. Lond. B Biol. Sci. 233, 137–175. https://doi.org/10.1098/rstb.1947.0008.
Pennington, W., 1943. Lake sediments: the bottom deposits of the north basin of Windermere, with special reference to the diatom succession. New Phytol. 42, 1–27.
Philippsen, B., 2013. The freshwater reservoir effect in radiocarbon dating. Herit. Sci. 1, 24. https://doi.org/10.1186/2050-7445-1-24.
Pinson, L.J.W., 2009. Derivation of Acoustic and Physical Properties from High-Resolution Seismic Reflection Data. PhD. University of Southampton.
Pinson, L.J.W., Vardy, M.E., Dix, J.K., Henstock, T.J., Bull, J.M., Maclachlan, S.E., 2013. Deglacial history of glacial lake Windermere, UK: implications for the central British and Irish Ice Sheet. J. Quat. Sci. 28, 83–94. https://doi.org/10.1002/jqs.2595.
Praeg, D., McCarron, S., Dove, D., Ó Cofaigh, C., Scott, G., Monteys, X., Facchin, L., Romeo, R., Coxon, P., 2015. Ice sheet extension to the celtic sea shelf edge at the last glacial maximum. Quat. Sci. Rev. 111, 107–112. https://doi.org/10.1016/j.quascirev.2014.12.010.
Rasmussen, S.O., Andersen, K.K., Svensson, A.M., Steffensen, J.P., Vinther, B.M., Clausen, H.B., Siggaard-Andersen, M.L., Johnsen, S.J., Larsen, L.B., Dahl-Jensen, D., Bigler, M., Röthlisberger, R., Fischer, H., Goto-Azuma, K., Hansson, M.E., Ruth, U., 2006. A new Greenland ice core chronology for the last glacial termination. J. Geophys. Res. Atmos. 111, 1–16. https://doi.org/10.1029/2005JD006079.
Rasmussen, S.O., Bigler, M., Blockley, S.P., Blunier, T., Buchardt, S.L., Clausen, H.B., Cvijanovic, I., Dahl-Jensen, D., Johnsen, S.J., Fischer, H., Gkinis, V., Guillevic, M., Hoek, W.Z., Lowe, J.J., Pedro, J.B., Popp, T., Seierstad, I.K., Steffensen, J.P., Svensson, A.M., Vallelonga, P., Vinther, B.M., Walker, M.J., Wheatley, J.J., Winstrup, M., 2014. A stratigraphic framework for abrupt climatic changes during the Last Glacial period based on three synchronized Greenland ice-core records: refining and extending the INTIMATE event stratigraphy. Quat. Sci. Rev. 106, 14–28. https://doi.org/10.1016/j.quascirev.2014.09.007.
Reimer, P., Bard, E., Bayliss, A., Beck, J.W., Blackwell, P.G., Bronk Ramsey, C., Buck, C.E., Cheng, H., Edwards, R.L., Friedrich, M., Grootes, P.M., Guilderson, T.P., Haflidason, H., Hajdas, I., Hatté, C., Heaton, T.J., Hoffmann, D.L., Hogg, A.G., Hughen, K.A., Kaiser, K.F., Kromer, B., Manning, S.W., Niu, M., Reimer, R.W., Richards, D.A., Scott, E.M., Southon, J.R., Staff, R.A., Turney, C.S.M., van der Plicht, J., 2013. IntCal13 and Marine13 radiocarbon age calibration curves 0–50,000 Years cal BP. Radiocarbon 55, 1869–1887. https://doi.org/10.2458/azu_js_rc.55.16947.
Ridge, J.C., Balco, G., Bayless, R.L., Beck, C.C., Carter, L.B., Dean, J.L., Voytek, E.B., Wei, J.H., 2012. The new north american varve chronology: a precise record of southeastern laurentide ice sheet deglaciation and climate, 18.2-12.5 KYR BP, and correlations with Greenland ice core records. Am. J. Sci. 312, 685–722. https://doi.org/10.2475/07.2012.01.
Ringberg, B., 1991. Late Weichselian Clay Varve Chronology and Glaciolacustrine Environment during Deglaciation in Southern Sweden (Uppsala).
Roberts, A.P., Chang, L., Christopher, J.R., Chorng-Shern, H., Florindo, F., 2011. Magnetic properties of sedimentary greigite (Fe3S4): an update. Rev. Geophys. 49, 1–46. https://doi.org/10.1029/2010RG000336.1.INTRODUCTION.
Roberts, D.H., Evans, D.J.A., Callard, S.L., Clark, C.D., Bateman, M.D., Medialdea, A., Dove, D., Cotterill, C.J., Saher, M., Ó Cofaigh, C., Chiverrell, R.C., Moreton, S.G., Fabel, D., Bradwell, T., 2018. Ice marginal dynamics of the last British-Irish ice sheet in the southern North sea: ice limits, timing and the influence of the Dogger bank. Quat. Sci. Rev. 198, 181–207. https://doi.org/10.1016/j.quascirev.2018.08.010.
Sissons, J., 1980. The loch lomond advance in The lake District, northern England. Trans. R. Soc. Edinb. 71, 13–27.
Small, D., Benetti, S., Dove, D., Ballantyne, C.K., Fabel, D., Clark, C.D., Gheorghiu, D.M., Newall, J., Xu, S., 2017a. Cosmogenic exposure age constraints on deglaciation and flow behaviour of a marine-based ice stream in western Scotland, 21–16 ka. Quat. Sci. Rev. 167, 30–46. https://doi.org/10.1016/j.quascirev.2017.04.021.
Small, D., Clark, C.D., Chiverrell, R.C., Smedley, R.K., Bateman, M.D., Duller, G.A.T., Ely, J.C., Fabel, D., Medialdea, A., Moreton, S.G., 2017b. Devising quality assurance procedures for assessment of legacy geochronological data relating to deglaciation of the last British-Irish Ice Sheet. Earth Sci. Rev. 164, 232–250. https://doi.org/10.1016/j.earscirev.2016.11.007.
Smedley, R.K., Chiverrell, R.C., Ballantyne, C.K., Burke, M.J., Clark, C.D., Duller, G.A.T., Fabel, D., McCarroll, D., Scourse, J.D., Small, D., Thomas, G.S.P., 2017a. Internal dynamics condition centennial-scale oscillations in marinebased ice-stream retreat. Geology 45, 787–790. https://doi.org/10.1130/G38991.1.
Smedley, R.K., Scourse, J.D., Small, D., Hiemstra, J.F., Duller, G.A.T., Bateman, M.D., Burke, M.J., Chiverrell, R.C., Clark, C.D., Davies, S.M., Fabel, D., Gheorghiu, D.M., McCarroll, D., Medialdea, A., Xu, S., 2017b. New age constraints for the limit of the British–Irish ice sheet on the Isles of Scilly. J. Quat. Sci. 32, 48–62. https://doi.org/10.1002/jqs.2922.
Smith, S.V., Bradley, R.S., Abbott, M.B., 2004. A 300 year record of environmental change from lake Tuborg, Ellesmere island, Nunavut, Canada. J. Paleolimnol. 32, 137–148. https://doi.org/10.1023/B:JOPL.0000029431.23883.1c.
Steffensen, J.P., Andersen, K.K., Bigler, M., Clausen, H.B., Dahl-Jensen, D., Fischer, H., Goto-Azuma, K., Hansson, M., Johnsen, S.J., Jouzel, J., Masson-Delmotte, V., Popp, T., Rasmussen, S.O., Röthlisberger, R., Ruth, U., Stauffer, B., Siggaard-Andersen, M.-L., Sveinbjörnsdóttir, A.E., Svensson, A., White, J.W.C., 2008. High-resolution Greenland ice core data show abrupt climate change happens in few years. Science 321, 680–684. https://doi.org/10.1126/science.1157707.
Stuiver, M., Reimer, P.J., 1993. Extended 14C data base and revised CALIB 3.0 14C age calibration program. Radiocarbon 35, 215–230.
Swiss Glacier Monitoring Network, 2017. Grosser Aletschgletscher [WWW Document]. http://swiss-glaciers.glaciology.ethz.ch/glaciers/aletsch.html (accessed 7.19.18).
Tipping, 1991. Climatic change in Scotland during the Devensian late glacial: the palynological record. In: Barton, N., Roberts, A.J., Roe, D.A. (Eds.), The Late Glacial in North-West Europe: Human Adaptation and Environmental Change at the End of the Pleistocene. Council for British Archaeology, London, pp. 7–21.
Tomkins, J.D., Lamoureux, S.F., Antoniades, D., Vincent, W.F., 2008. Sedimentary pellets as an ice-cover proxy in a High Arctic ice-covered lake. J. Paleolimnol. 41,

225–242. https://doi.org/10.1007/s10933-008-9255-x.
Tomkins, M.D., Dortch, J.M., Hughes, P.D., 2017. Erratum to: "Tomkins et al. (2016) Schmidt Hammer exposure dating (SHED): establishment and implications for the retreat of the last British Ice Sheet" [Quat. Geochronol. (2016) 33 (46–60)] (S1871101416300085)(10.1016/j.quageo.2016.02.002). Quat. Geochronol. 38, 75–76. https://doi.org/10.1016/j.quageo.2016.11.003.
Tomkins, M.D., Dortch, J.M., Hughes, P.D., 2016. Schmidt Hammer exposure dating (SHED): establishment and implications for the retreat of the last British Ice Sheet. Quat. Geochronol. 33, 46–60. https://doi.org/10.1016/j.quageo.2016.02.002.
Tomkins, M.D., Dortch, J.M., Hughes, P.D., Huck, J.J., Tonkin, T.N., Barr, I.D., 2018. Timing of glacial retreat in the Wicklow Mountains, Ireland, conditioned by glacier size and topography. J. Quat. Sci. 33, 611–623. https://doi.org/10.1002/jqs.3040.
Turner, G.M., Thompson, R., 1981. Lake sediment record of the geomagnetic secular variation in Britain during Holocene times. Geophys. J. Int. 65, 703–725. https://doi.org/10.1111/j.1365-246X.1981.tb04879.x.
Vardy, M.E., Pinson, L.J.W., Bull, J.M., Dix, J.K., Henstock, T.J., Davis, J.W., Gutowski, M., 2010. 3D seismic imaging of buried Younger Dryas mass movement flows: lake Windermere, UK. Geomorphology 118, 176–187. https://doi.org/10.1016/j.geomorph.2009.12.017.
Wilson, C., 1987. The outflow of Windermere, Cumbria: a re-appraisal. Geol. J. 22, 219–224.
Wilson, P., 2004. Description and implications of valley moraines in upper Eskdale, Lake District. Proc. Geol. Assoc. 115, 55–61.
Wilson, P., Ballantyne, C.K., Benetti, S., Small, D., Fabel, D., Clark, C.D., 2019. Deglaciation chronology of the Donegal ice centre, north-west Ireland. J. Quat. Sci. 34, 16–28. https://doi.org/10.1002/jqs.3077.
Wilson, P., Clark, R., 1998. Characteristics and implications of some Loch Lomond Stadial moraine ridges and later landforms, eastern Lake District, northern England. Geol. J. 2, 73–87.
Wilson, P., Lord, T., 2014. Towards a robust deglacial chronology for the northwest England sector of the last British-Irish Ice Sheet. North West Geogr. 14, 1–11.
Wilson, P., Rodés, Á., Smith, A., 2018. Valley glaciers persisted in the Lake District, north-west England, until ~16–15 ka as revealed by terrestrial cosmogenic nuclide (10Be) dating: a response to Heinrich event 1? J. Quat. Sci. 33, 518–526. https://doi.org/10.1002/jqs.3030.
Wilson, P., Schnabel, C., Wilcken, K.M., Vincent, P.J., 2013. Surface exposure dating (36Cl and 10Be) of post-Last Glacial Maximum valley moraines, Lake District, northwest England: some issues and implications. J. Quat. Sci. 28, 379–390. https://doi.org/10.1002/jqs.2628.
Wohlfarth, B., 1996. The chronology of the last termination: a review of radiocarbon-dated, high-resolution terrestrial stratigraphies. Quat. Sci. Rev. 15, 267–284. https://doi.org/10.1016/0277-3791(96)00001-7.
Wohlfarth, B., Björck, S., Holmqvist, B., Lemdahl, G., Ising, J., 1994. Ice recession and depositional environment in the Blekinge archipelago of the Baltic ice lake. GFF 116, 3–12. https://doi.org/10.1080/11035899409546134.
Wu, Y., Li, S., Lücke, A., Wünnemann, B., Zhou, L., Reimer, P., Wang, S., 2010. Lacustrine radiocarbon reservoir ages in Co Ngoin and Zigê Tangco, central Tibetan plateau. Quat. Int. 212, 21–25. https://doi.org/10.1016/j.quaint.2008.12.009.
Zolitschka, B., 2007. Varved lake sediments. In: Elias, S.A. (Ed.), Encyclopedia of Quaternary Science. Elsevier, pp. 3105–3114. https://doi.org/10.1016/B0-444-52747-8/00065-X.
Zolitschka, B., 1996. Recent sedimentation in a high arctic lake, northern Ellesmere Island, Canada. J. Paleolimnol. 16, 169–186.
Zolitschka, B., Francus, P., Ojala, A.E.K., Schimmelmann, A., 2015. Varves in lake sediments – a review. Quat. Sci. Rev. 117, 1–41. https://doi.org/10.1016/j.quascirev.2015.03.019.
Dean, J., Kemp, A.E.S., Bull, D., Pike, J., 1999. Taking varves to bits: scanning electron microscopy in the study of laminated sediments and varves. J. Paleolimnol. 22, 121–136.
Kemp, A.E.S., Pearce, R.B., Pike, J., Marshall, J.E.A., 1998. Microfabric and micro-compositional studies of pliocene and quaternary sapropels from the eastern Mediterranean. Proc. Ocean Drill. Program Sci. Results 160, 349–364.
Pike, J., Kemp, A.E.S., 1996. Preparation and analysis techniques for studies of laminated sediments. Geol. Soc. Lond. Spec. Publ. 116, 37–48. https://doi.org/10.1144/GSL.SP.1996.116.01.05.